Modelling winter organic aerosol at the European scale with CAMx: evaluation and source apportionment with a VBS parameterization based on novel wood burning smog chamber experiments

Giancarlo Ciarelli[1,a], Sebnem Aksoyoglu[1], Imad El Haddad[1], Emily A. Bruns[1], Monica Crippa[2], Laurent Poulain[3], Mikko Äijälä[4], Samara Carbone[5], Evelyn Freney[6], Colin O'Dowd[7], Urs Baltensperger[1] and André S. H. Prévôt[1]

[1]{Paul Scherrer Institute, Laboratory of Atmospheric Chemistry, 5232 Villigen PSI, Switzerland}

[2]{European Commission, Joint Research Centre (JRC), Directorate for Energy, Transport and Climate, Air and Climate Unit, Via E. Fermi 2749, I-21027 Ispra (VA), Italy}

[3]{Leibniz-Institute for Tropospheric Research (TROPOS), Permoserstr. 15, 04318 Leipzig, Germany}

[4]{University of Helsinki, Department of Physics, Helsinki, Finland}

[5]{Institute of Physics, University of São Paulo, Rua do Matão Travessa R, 187, 05508-090 São Paulo, S.P., Brazil}

[6]{Laboratoire de Météorologie Physique (LaMP), CNRS/Université Blaise Pascal, Clermont-Ferrand, France}

[7]{School of Physics and Centre for Climate & Air Pollution Studies, Ryan Institute, National University of Ireland Galway, University Road, Galway, Ireland}

[a] now at: {Laboratoire Inter-Universitaire des Systèmes Atmosphériques (LISA), UMR CNRS 7583, Université Paris Est Créteil et Université Paris Diderot, Institut Pierre Simon Laplace, Créteil, France}

Correspondence to: S. Aksoyoglu (sebnem.aksoyoglu@psi.ch)

Abstract

We evaluated a modified VBS (Volatility Basis Set) scheme to treat biomass burning-like organic aerosol (BBOA) implemented in CAMx (Comprehensive Air Quality Model with extensions). The updated scheme was parameterized with novel wood combustion smog chamber experiments using a hybrid VBS framework that accounts for a mixture of wood burning organic aerosol precursors and their further functionalization and fragmentation in the atmosphere. The new scheme was evaluated for one of the winter EMEP intensive campaigns (February-March 2009) against aerosol mass spectrometer (AMS) measurements performed at 11 sites in Europe. We found a considerable improvement for the modelled organic aerosol (OA) mass compared to our previous model application with the mean fractional bias (MFB) reduced from -61% to -29%.

We performed model-based source apportionment studies and compared results against positive matrix factorization (PMF) analysis performed on OA AMS data. Both model and observations suggest that OA was mainly of secondary origin at almost all sites. Modelled secondary organic aerosol (SOA) contributions to total OA varied from 32 to 88% (with an average contribution of 62%) and absolute concentrations were generally under-predicted. Modelled primary hydrocarbon-like organic aerosol (HOA) and primary biomass burning-like aerosol (BBPOA) fractions contributed to a lesser extent (HOA from 3 to 30%, and BBPOA from 1 to 39%) with average contributions of 13 and 25%, respectively. Modelled BBPOA fractions was found to represent 12 to 64% of the total residential heating related OA, with increasing contributions at stations located in the northern part of the domain.

Source apportionment studies were performed to assess the contribution of residential and non-residential combustion precursors to the total SOA. Non-residential combustion and road transportation sector contributed about 30-40% to SOA formation (with increasing contributions at urban and near industrialized sites) whereas residential combustion (mainly related to wood burning) contributed to a larger extent, around 60-70%. Contributions to OA from residential combustion precursors in different volatility ranges were also assessed: our results indicate that residential combustion gas-phase precursors in the semivolatile range (SVOC) contributed from 6 to 30%, with higher contributions predicted at stations located in the southern part of the domain. On the other hand, the oxidation products of higher volatility

precursors (the sum of IVOCs and VOCs) contribute from 15 to 38% with no specific gradient among the stations.

Although the new parameterization leads to a better agreement between model results and observations, it still under-predicts the SOA fraction suggesting that uncertainties in the new scheme and other sources and/or formation mechanisms remain to be elucidated. Moreover, a more detailed characterization of the semivolatile components of the emissions is needed.

1 Introduction

Organic aerosol (OA) comprises the main fraction of fine particulate matter (PM_1) (Jimenez et al., 2009). Even though the sources of its primary fraction (primary organic aerosol, POA) are nominally known, uncertainties remain in terms of the total emission fluxes annually released into the troposphere (Kuenen et al., 2014). Moreover, the measured OA load largely exceeds the emitted POA fractions at most measurement sites around the world. A secondary fraction (SOA), formed from the condensation of oxidized gases with low-volatility on pre-existing particles, is found to be the dominant fraction of OA (Crippa et al., 2014; Huang et al., 2014; Jimenez et al., 2009). Such low-volatility products are produced in the atmosphere when higher volatility organic gases are oxidized by ozone (O_3), hydroxyl (OH) radical and/or nitrate (NO_3) radical. The physical and chemical processes leading to the formation of SOA are numerous, e.g. oxidation and condensation, oligomerization or aqueous-phase formation, and they are very uncertain and currently under debate (Hallquist et al., 2009; Tsigaridis et al., 2014; Fuzzi et al., 2015; Woody et al., 2016). Moreover, the solubility of organic compounds in water is also a crucial parameter affecting the life time of organic particles and gases in the atmosphere (Hodzic et al., 2016).

Available long-term measurements might help in elucidating the composition and origin of OA in different seasons. Canonaco et al. (2015) presented direct evidence for significant changes in the SOA fingerprint between summer and winter from 13 months of OA measurements conducted in Zürich using the aerosol chemical speciation monitor (ACSM). Their results indicate that summer oxygenated OA mainly arises from biogenic precursors whereas winter oxygenated OA is more strongly influenced by wood burning emissions. Moreover, numerous ambient studies with aircraft of open biomass burning plumes do not show a net increase in OA, despite observed oxidation (Cubison et al., 2011; Jolleys et al., 2012). It is therefore necessary that the chemical transport models (CTMs) correctly reproduce OA concentrations by taking into account all the uncertainties and variability of observations.

Most of the CTMs today account for SOA formation from biogenic and anthropogenic high volatility precursors such as terpenes, isoprene, xylene and toluene which have a saturation concentration (C^*) higher than 10^6 μg m^{-3} (Aksoyoglu et al., 2011; Ciarelli et al., 2016a). A few models also include intermediate volatility organic compounds (IVOCs) with a C^* of 10^3

- 10^6 μg m^{-3} and semivolatile organic compounds (SVOCs) with a C^* of 0.1 - 10^3 μg m^{-3} co-emitted with POA (Bergström et al., 2012; Ciarelli et al., 2016a; Denier van der Gon et al., 2015; Fountoukis et al., 2014; Tsimpidi et al., 2010; Woody et al., 2016). In these applications, the volatility distributions of POA and IVOCs emissions are based on the study of Robinson et al. (2007), where the IVOC mass is assumed to be 1.5 times the total organic mass available in the semivolatile range.

The standard gridded emission inventories do not yet include SVOCs and their emissions are still highly uncertain as their measurement is strongly affected by the method used (Lipsky and Robinson, 2006). A recent study by Denier van der Gon et al. (2015) reported a new residential wood burning emission inventory including SVOCs, where emissions are higher by a factor of 2-3 on average than those in the EUCAARI inventory (Kulmala et al., 2011). The new emission inventory was used in two CTMs (EMEP and PMCAMx) and it improved the model performance for the total OA (Denier van der Gon et al., 2015). Ciarelli et al. (2016a) showed that allowing for evaporation of primary organic particles as available in the European emission inventories degraded the model performance for the total OA mass (further under-predicted OA but the POA to SOA ratio in a better agreement with measurements). In the same study, on the other hand, model performance improved when volatility distribution that implicitly accounts for missing semivolatile material (increasing POA emissions by a factor of 3) was deployed.

Various modelling studies were performed by increasing POA emissions by a factor of 3 to compensate for the missing gaseous emissions based on partitioning theory predictions (Ciarelli et al., 2016a; Fountoukis et al., 2014; Shrivastava et al., 2011; Tsimpidi et al., 2010). Fig. S1 shows the partitioning of ~1 μg m^{-3} of POA at different temperatures using the latest available volatility distribution for biomass burning (May et al., 2013). The ratio between the available gas and particle phase material in the semivolatile range is predicted to be roughly 3. This implies that, in these applications, the new emitted organic mass (POA + SVOCs + IVOCs) is 7.5 times higher than in original emissions (i.e., OM = (3*POA) + (1.5*(3*POA))) which could be used as an indirect method to account for missing organic material in the absence of more detailed gridded emission inventories.

Along with ambient measurement studies, novel wood burning smog chamber studies provide more insight into wood burning SOA formation and the nature of its precursors. Bruns et al.

(2016) performed several wood-burning aging experiments in a ~7 m^3 smog chamber. Using proton-transfer-reaction mass spectrometry (PTR-MS) they characterized SOA precursors at the beginning of each aging experiment and found that up to 80% of the observed SOA could be explained with a collection of a few SOA precursors that are usually not accounted in regional CTMs (e.g. cresol, phenol, naphthalene). Recently, we used those chamber data to parameterize a hybrid volatility basis set (Ciarelli et al., 2016b). The results provided new direct information regarding the amount of wood burning SOA precursors which could be directly used in CTM applications in the absence of more refined wood burning emissions in gridded inventories. The box-model application reproduced the chamber data with an error of approximately 25% on the OA mass and 15% on the O:C ratio (Ciarelli et al., 2016b).

In the current study, the updated volatility basis set (VBS) parameterization was implemented in the comprehensive air quality model with extensions (CAMx) model, and simulations were performed in Europe for a winter period in February-March 2009. Results are compared with previous simulations using the original VBS framework (Ciarelli et al., 2016a) and with source apportionment data at eleven sites with different exposure characteristics, obtained using PMF applied to AMS measurements (Crippa et al., 2014).

2 Method

2.1 Regional modelling with CAMx

The CAMx version 5.41 with VBS scheme (ENVIRON, 2011; Koo et al., 2014) was used in this study to simulate an EMEP measurement campaign between 25 February and 26 March 2009 in Europe. The modelling method and input data were the same as those used in the EURODELTA III (ED III) project, described in detail in Ciarelli et al. (2016a). The model domain covers Europe with a horizontal resolution of 0.25° x 0.25°. Meteorological parameters were calculated from ECMWF IFS (Integrated Forecast System) data at 0.2° resolution. There were 33 terrain-following σ-levels from ~20 m above ground level (first layer) up to about 350 hPa, as in the original IFS data. For the gas phase chemistry, the Carbon Bond (CB05) mechanism (Yarwood, 2005). The ISORROPIA thermodynamic model (Nenes et al., 1998) was used for the partitioning of inorganic aerosols (sulfate, nitrate, ammonium, sodium and chloride). Aqueous sulfate and nitrate formation in cloud water was calculated using the RADM algorithm (Chang et al., 1987). Formation and evolution of OA is

156 treated with a hybrid volatility basis set (VBS) that accounts for changes in volatility and O:C
157 ratio (Koo et al., 2014) with dilution and aging. Particle size distributions were treated with a
158 two static mode scheme (fine and coarse). The results presented in this study refer to the fine
159 fraction ($PM_{2.5}$). We parameterized the biomass burning sets based on chamber data as
160 described in Ciarelli et al. (2016b).

161 The anthropogenic emission inventory was made available for the ED III community team by
162 the National Institute for Industrial Environment and Risks (INERIS) at 0.25° x 0.25°
163 horizontal resolution. More information regarding the anthropogenic emission inventories are
164 available in Bessagnet et al. (2014, 2016) and Ciarelli et al. (2016a). Hourly emissions of
165 biogenic VOCs, such as monoterpenes, isoprene, sesquiterpenes, xylene and toluene, were
166 calculated using the Model of Emissions of Gases and Aerosols from Nature MEGANv2.1
167 (Guenther et al., 2012) for each grid cell in the model domain.

168 ## 2.2 Organic aerosol scheme

169 The biomass burning organic aerosol scheme was constrained using recently available wood
170 burning smog chamber data (Bruns et al., 2016) as described in Ciarelli et al. (2016b). The
171 model deploys three different basis sets (Donahue et al., 2011) to simulate the emissions of
172 organics from biomass burning and their evolution in the atmosphere. The first set allocates
173 fresh emissions into five volatility bins with saturation concentrations ranging between 10^{-1}
174 and 10^{3} μg m^{-3} following the volatility distribution and enthalpy of vaporization proposed by
175 May et al. (2013). In order to include gas-phase organics in the semivolatile range in the
176 absence of more detailed inventory data, we used the approach of increasing the standard
177 emissions by a factor of 3 proposed by previous studies (Shrivastava et al., 2011; Tsimpidi et
178 al., 2010) which is also in line with the recent European study on the revision of the
179 residential wood combustion emissions (Denier van der Gon et al., 2015). This approach of
180 including the semivolatile compounds can be used until detailed emission inventories with
181 more realistic inter-country distribution of the emissions become available (e.g. Denier van
182 der Gon et al., 2015). The second set allocates oxidation products from SVOCs after shifting
183 the volatility by one order of magnitude. The third set allocates oxidation products from the
184 traditional VOCs and biogenic precursors (xylene, toluene, isoprene, monoterpenes and
185 sesquiterpenes) and from non-traditional SOA precursors retrieved from chamber data (~4.75

times the amount of organic material in the semivolatile range, Ciarelli et al., 2016b). Primary and secondary semivolatile compounds react with OH in the gas-phase with a rate constant of 4×10^{-11} cm^3 $molec^{-1}$ s^{-1} (Donahue et al., 2013), which decreases their saturation concentration by one order of magnitude. This implies that also aging of biogenic products is implicitly taken into account.

A reaction rate of 4 x $10^{-11}cm^3molec^{-1}s^{-1}$ was also applied to the rest of the anthropogenic sources (referred to as HOA) in order to be consistent among all the other anthropogenic sources as already proposed by more recent studies for the range of saturation concentrations used here (Donahue et al., 2013). No heterogeneous oxidation of organic particles or oligomerization processes is included in the model. The new model parameterization described in this study is referred to as VBS_BC_NEW throughout the paper to distinguish it from the previous base case called VBS_BC as given in Ciarelli et al. (2016a). All the VBS sets are listed in Table 1. More detailed on the VBS scheme can be found in Ciarelli et al. (2016b) and Koo et al. (2014).

2.3 Model evaluation

The model results for the period between 25 February and 26 March 2009 were compared with OA concentrations measured by AMS at 11 European sites. Modelled BBPOA, HOA and SOA concentrations were compared with multi-linear engine 2 (ME-2) analysis performed on AMS data (Paatero, 1999) using source finder (SoFi) (Canonaco et al., 2013; Crippa et al., 2014). Elevated sites such as Montseny and Puy de Dôme were also included in the analysis and modelled concentrations for these two sites were extracted from higher layers in order to minimize the artefacts due to topography in a terrain-following coordinate system. This was not the case in our previous application, where model OA concentrations were extracted from the surface layer (Ciarelli et al., 2016a). We assumed OA emissions from SNAP2 (emissions from non-industrial combustion plants in the Selected Nomenclature for Air Pollution) and SNAP10 (emissions from agriculture, about 6% of POA in SNAP2), to be representative of biomass burning emissions and thus comparable to the BBPOA PMF factor. OA from all other SNAP categories were compared against HOA-like PMF factors. Unfortunately, gridded emissions for SNAP2 include other emission sources (i.e., coal burning which might be important in eastern European countries like Poland). We could not

resolve our emission inventory with sufficient detail to separate the contribution of coal for these European cites (Crippa et al., 2014). Finally, the SOA fraction was compared to the PMF-resolved oxygenated organic aerosol (OOA) fraction.

Statistics were reported in terms of mean bias (MB), mean error (ME), mean fractional bias (MFB), mean fractional error (MFE) and coefficient of determination (R^2) (see Table S1 for the definition of statistical parameters).

3 Results and discussions

3.1 Analysis of the modelled OA

Figure 1 shows the average modelled OA concentrations and surface temperature for the period between 25 February and 26 March 2009. Temperatures were below 0°C in the north, ranged 5-10°C in central Europe and were above 10°C in the southern part of the domain. Model performance for surface temperature was evaluated within the ED III exercise and found to be reproduced reasonably well, with a general under-prediction of around 1°C (Bessagnet et al., 2014).

A clear spatial variability in the modelled OA concentrations is observed (Fig. 1). Predicted OA concentrations were higher in eastern European countries (especially Romania and southern Poland) as well as over northern Italy (8-10 μg m^{-3} on average) whereas they were lower in the northern part of the domain. A similar spatial distribution of OA concentrations was also reported by Denier van der Gon et al. (2015) using the EMEP model. Relatively high OA concentrations over the Mediterranean Sea are mainly of secondary origin due to enhanced photochemical activity (more details are found in Section 3.2). In addition, the reduced deposition efficiency over water leads to higher OA levels.

The scatter plots in Fig. 2 show the modelled (VBS_BC_NEW) versus measured daily average OA concentrations at 11 sites in Europe together with the results from our previous model application (VBS_BC, Ciarelli et al., 2016a) for comparison. The modified VBS scheme (VBS_BC_NEW) predicts higher OA concentrations compared to our previous study using the original scheme (VBS_BC) (~ 60% more OA on average at all sites). Statistical parameters improved significantly (Table 2); the mean fractional bias MFB decreased from -61% in VBS_BC to -29% in VBS_BC_NEW and the model performance criteria were met

(Boylan and Russell, 2006). The coefficient of determination remained almost unchanged for OA in the VBS_BC_NEW case (R^2=0.58) compared to VBS_BC (R^2=0.57) indicating that the original model was able to similarly capture the OA daily variation, but not its magnitude. Improvements in the modelled SOA fraction were also observed using the original VBS approach (Koo et al., 2014) when aging of the biomass burning vapours were taken into account (Fig. S4). The majority of the stations show an $R^2 \geq 0.4$. Lower values were found for the elevated sites of Montseny and Puy de Dome (R^2=0.17 and R^2=0.13, respectively) and also at the Helsinki site (R^2=0.06). In spite of the improvements with respect to earlier studies, modelled OA is still lower than measured (mean bias MB from -0.1 μg m^{-3} up to -3.1 μg m^{-3}) at most of the sites, with only a slight overestimation at a few locations (MB from 0.3 μg m^{-3} up to 0.9 μg m^{-3}).

The observed OA gradient among the 11 sites was reproduced very well (R^2 = 0.72) (Fig. 3). Both measured and modelled OA concentrations were highest in Barcelona. Other sites with concentrations greater than 2 μg m^{-3} were Payerne, Helsinki, Vavihill and Montseny. Barcelona and Helsinki are both classified as urban stations, which justifies the higher OA loads due to the anthropogenic activities (e.g. traffic, cooking and heating). Anthropogenic activities in the area of Barcelona could also affect OA concentrations at Montseny which is about 40 km away. In the case of Payerne and Vavihill, the relatively high OA concentrations might be due to residential heating, where wood is largely used as a combustion fuel during cold periods (Denier van der Gon et al., 2015). For Chilbolton, located not far from London, this might not be the case: the fuel wood usage in the UK is the lowest in Europe (Denier van der Gon et al., 2015). Ots et al. (2016) suggested the possibility of missing diesel-related IVOCs emissions, which might be an important source of SOA in those regions. However, other studies reported substantial contribution from solid fuel combustion to OA (Young et al., 2015). In this case, it might be that difficulties in reproducing the OA concentration are mainly related to the relatively complex area of the site (i.e., close to the English Channel). An evaluation of diurnal variations of HOA and SOA concentrations for this site showed a consistent under-prediction of both components (Fig. S2).

3.2 Analysis of the OA components

The predicted POA spatial distribution (Fig. 4) resembles the residential heating emission pattern of different countries (Bergström et al., 2012). The highest POA concentrations were predicted in east European countries, France, Portugal and in northern Italy (~3-5 μg m^{-3}) whereas they were less than 1 μg m^{-3} in the rest of the model domain. Very low OA concentrations in Sweden were already shown by previous European studies. Bergström et al. (2012) reported that emissions of organic carbon (OC) from the residential heating sector in Sweden were lower than those in Norway by a factor of 14 in spite of its higher wood usage by 60%. This indicates an underestimation of emissions from residential heating in the emission inventory. The spatial distribution of SOA concentrations, on the other hand, is more widespread with a visible north to south gradient (Fig. 4). Higher SOA concentration were predicted close to primary emission sources (e.g. Poland, Romania, Po Valley and Portugal) but also in most of the countries below 50° latitude and over the Mediterranean Sea where higher OH concentration, reduced deposition efficiency and high contribution from long-range transport are expected (average concentrations around 3-4 μg m^{-3}).

Comparison of results from this study (VBS_BC_NEW) with the earlier one (VBS_BC, Ciarelli et al., 2016a) suggests that the new VBS scheme predicts higher SOA concentrations by about a factor of 3 (Fig. 5) and improves the model performance when comparing assessed OOA from measurements with modelled SOA (Table 4). POA concentrations, on the other hand, are clustered below 1 μg m^{-3} except in Barcelona (Fig. 5), showing an R^2=0.36 (Table 3). Although predicted POA concentrations at Barcelona were lower than the measurements, MFB=-47% and MFE=69% were still in the range for acceptable performance criteria (MFE ≤+75% and −60 < MFB < + 60 %, Boylan and Russell, 2006). On the other hand, the model over-predicted the POA concentrations at Hyytiälä (MFB=131% and MFE=131%), Helsinki (MFB=95% and MFE=100%) and Cabauw (MFB=76% and MFE=86%) mainly due to the overestimated BBPOA fraction as seen in Fig. 6.

At most of the sites, OA was dominated by SOA (Fig. 6 and Fig. 7) which was underestimated in particular at Chilbolton, Melpitz and Vavihill (Table 4). As already mentioned, the under-prediction of SOA concentrations might be attributed to missing SOA precursors or uncertainties in SOA formation mechanisms and removal processes. On the other hand, the remote station of Mace Head showed a positive bias for SOA (MFB = 30%),

even though model and measurement concentrations were very similar (0.54 and 0.35 μg m^{-3}, respectively), which could be attributed to an overestimated contribution from the boundaries. The relatively small positive bias at the two elevated sites, Montseny and Puy de Dome (MFB = 4% and 17%, respectively), is most likely the result of difficulties in capturing the inversion layer, as confirmed by the over-prediction of other PM species at these sites (Fig. S3).

Mostly traffic-related HOA was underestimated at the urban site Barcelona (Table S2, Fig. 6), with the model not able to reproduce the diurnal variation of HOA at this urban site likely due to poorly reproduced meteorological conditions or too much dilution during day time in the model (Fig. S2). The under-prediction of the HOA fraction is consistent with our previous study where model evaluation for NO_2 revealed a systematic under-estimation of the modelled concentration (Ciarelli et al., 2016a). The coarse resolution of the domain (0.25° x 0.25°) may result in too low emissions especially at urban sites. In addition, the gridded emission inventories still represent a large source of uncertainties for CTM applications. The majority of the NO_x ($NO+NO_2$) emissions in Europe arises from the transportation sector (SNAP7), which might have much larger uncertainties than previously thought (Vaughan et al., 2016). An evaluation of planetary boundary layer height (PBLH) within the EDIII shows that although the PBLH was quite well represented in general in the ECMWF IFS meteorological fields, CAMx tends to underestimate the night-time minima and to overestimate some daytime peaks. The other urban site considered in this study is Helsinki. In this case, HOA concentrations were over-predicted, as seen in Figs. 6 and S2, which might indicate missing dispersion processes in the model or under-estimated dilution.

The modelled BBPOA fraction on the other hand was generally overpredicted as in our previous application (Table S4), with an average MFB of 50% (Table S3, Figs. 6-7), which might arise from various factors: 1) In the model, POA emissions from SNAP2 and SNAP10 are assumed to be representative of BBPOA emissions which might not be the case for all European countries (other non-wood fuels such as coal, which is allocated to SNAP2 category and could not be separated in this study), 2) The under-prediction of the modelled surface temperature (Bessagnet et al., 2014) will directly influence the partitioning of organic material in the semivolatile range, favouring freshly emitted organic material to condense more to the particle phase, 3) Uncertainties in the adopted volatility distributions and/or in the oxidation processes of semivolatile organic vapours, 4) The simplistic way of accounting for the

semivolatile part of primary emissions might lead, in some areas, to the double counting of such compounds 5) Uncertainties in the retrieved BBPOA fraction from PMF analysis.

The temporal variability of OA concentrations was reproduced quite well (Fig. 8); the magnitudes of only a few (Vavihill, Chilbolton and Barcelona) were underestimated. Diurnal variations of HOA, BBPOA and SOA components at the rural-background sites suggest that the model was able to reproduce the relatively flat profile of the measured SOA and the increased BBPOA concentrations at night (Fig. 9). On the other hand, there was a slight underestimation of HOA during the day, especially around noon, possibly as a result of too much dilution in the model.

In our previous application, we performed a sensitivity study with increased biogenic and residential heating emissions by a factor of two (Ciarelli et al., 2016a). While the model was rather insensitive to the increased biogenic emissions during winter periods, a substantial increase in the OA concentrations was observed when emissions from residential heating were doubled. The model with doubled emissions from residential heating (VBC_BC_2xBBOA), overestimated the POA fraction at most of the sites (Fig. 10) with smaller effects on SOA, even though a better closure was achieved between modelled and observed OA. The results of the simulations using the new parameterization (VBC_BC_NEW), on the other hand, were closer to the measurement data especially for the SOA fraction (Fig. 10).

3.3 Residential versus non-residential combustion precursors

More detailed source apportionment studies were performed in order to assess the importance of residential and non-residential combustion precursors for OA and SOA. The upper panel in Fig. 11 shows the relative contributions to SOA from residential and non-residential combustion precursors. The model results indicate that non-residential combustion and transportation precursors contribute to about 30-40 % of the SOA formation (with increasing contribution at urban and near-industrialized sites) whereas residential combustion (mainly related to wood burning) contributes to a larger extent, i.e., around 60-70%. The residential combustion precursors were further apportioned to semivolatile and higher volatility precursors (Fig. 11, lower panel). In particular, SVOC precursors exhibit a south-to-north gradient with increasing contribution to the residential heating related OA for stations located

in the southern part of the domain (maximum and minimum contributions of 42 and 17% in Montseny and Hyytiälä, respectively). Such a gradient also reflects the effect of temperature on the partitioning of semivolatile organic material: the lower temperatures in the northern part of the domain will reduce the saturation concentration of the organic compounds allowing primary organic material to favour the particle phase and reducing the amount of SVOCs available that could act as SOA precursors. In the southern part of the domain, where more OH is available, the higher temperature will favour more organic material in the semivolatile range to reside in the gas-phase, rendering it available for oxidation. On the other hand, no south-to-north gradient was predicted for the SOA formed from the higher volatility class of precursors. Source apportionment for different volatilities classes of the non-residential and transportation sectors is currently not implemented for this model application. Since biogenic SOA is included in the same set as the biomass burning (set3) for this model application, we performed a sensitivity test with no SOA formation from biogenic precursors (where the reactions of isoprene, monoterpene and sesquiterpene with OH, O3 and NO3 were turned off). Our results indicated that for this period, biogenic precursors contribute to SOA to a lesser extent (5-20%) than the anthropogenic ones, with higher contributions at southern stations consistent with higher temperatures, and consequently more biogenic emissions compared to the northern stations (Fig. S5). The most predominant source was still predicted to be anthropogenic. Snow cover for March 2009 as retrieved from the TERRA/MODIS revealed that larger parts of the Scandinavian countries were almost completely covered with snow (Fig. S6), partially suppressing the emission of biogenic precursors and in line with very low contribution predicted from biogenic sources in Helsinki and Hyytiälä. Comparison of SOA from VBS_BC_NEW and the sensitivity test with no biogenic SOA formation showed similar improvement with respect to VBS_BC, with differences occurring mainly in the southern stations of Barcelona and Montseny (Fig. S7).

A comprehensive summary of the contribution to the total OA from all the sources (i.e. HOA, BBPOA, residential combustion semivolatile precursors, residential combustion higher volatility precursors and non-residential combustion precursors) is shown in Fig. 12 at each of the measurement sites. Residential combustion precursors in the semivolatile range contributed from 6 to 30% whereas higher volatility compounds contributed to a larger extent, i.e. from 15 to 38%. SOA from non-residential combustion precursors contributed from 10 to

37% to the total OA. The primary sources HOA and BBPOA contributed from 3 to 30% and 1-39%, respectively. These results lead to the conclusion that the overall contribution of residential combustion to OA concentrations in Europe varies between 52% at stations in the UK and 75-76% at stations in Scandinavia.

Conclusion

This study aims to evaluate recent VBS parameterizations in commonly used CTMs and to underline the importance of taking into account updated and more detailed SOA schemes as new ambient and chamber measurements elucidate the high complexity and strong variability of OA. In this context, a new VBS parameterization (based on recent wood burning experiments) implemented in CAMx was evaluated against high-resolution AMS measurements at 11 sites in Europe during February-March 2009, one of the winter EMEP intensive measurement campaigns. Results obtained from this study were compared with those from our earlier work in which the original VBS scheme in CAMx was applied. A detailed source apportionment for the organic aerosol (OA) fraction was discussed. This study provided the following outcome:

- A considerable improvement was found for the modelled OA concentrations compared to our previous studies mainly due to the improved secondary organic aerosol (SOA) performance. The average bias for the 11 AMS sites decreased by about 60% although the model still underestimates the SOA fraction.

- Both model and PMF source apportionment based on measurements suggested that OA was mainly of secondary origin with smaller primary contribution, with primary contribution of 13 and 25% for HOA and BBPOA, respectively. Predicted HOA concentrations were in the range of those retrieved from the PMF analysis at most of the sites except at the urban Barcelona site which could be related to the uncertainties in emissions or too much dilution in the model. On the other hand, the modelled BBPOA was higher than the measurements at several stations indicating the need for further studies on residential heating emissions, their volatility distribution and oxidation pathway of the semivolatile organic gases. In addition, more detailed emission inventories are needed to characterize the semivolatile components better, as proposed by Denier van der Gon et al. (2015).

- Emissions from the residential heating sector (SNAP2) largely influenced the OA composition. The modeled primary BBPOA fraction contributed from 46% to 77% of the total primary organic fraction (POA), with an average contribution of 65%. Non-residential combustion and transportation precursors contributed about 30-40% to SOA (with increasing contribution at urban and near-industrialized sites) whereas residential combustion (mainly related to wood burning) contributes to a larger extent, ~ 60-70%. Moreover, the contribution to OA from residential combustion precursors in different range of volatilities was also investigated: residential combustion gas-phase precursors in the semivolatile range contributed from 6 to 30% with a positive south-to-north gradient. On the other hand, higher volatility residential combustion precursors contributed from 15 to 38% showing no specific gradient among the stations.
- Model simulations performed with and without biogenic SOA formation revealed that, for this period, biogenic SOA contributed only to a small extent to the total SOA (5-20%), with an increasing gradient from north to south.

Acknowledgements

We thank the EURODELTA III modelling community, especially INERIS, TNO as well as ECMWF for providing various model input data. Calculations of land use data were performed at the Swiss National Supercomputing Centre (CSCS). We thank D. Oderbolz for developing the CAMxRunner framework to ensure reproducibility and data quality among the simulations and sensitivity tests. M. Tinguely for the visualization software, and RAMBOLL ENVIRON for their valuable comments. This study was financially supported by the Swiss Federal Office of Environment (FOEN). The research leading to these results received funding from the European Community's Seventh Framework Programme (FP7/2007-2013) under grant agreement no. 290605 (PSI-FELLOW), from the Competence Center Environment and Sustainability (CCES) (project OPTIWARES) and from the Swiss National Science Foundation (WOOSHI grant 140590). We thank D.A. Day for analysis on the DAURE dataset. Erik Swietlicki for the Vavihill dataset, Claudia Mohr for the Barcelona dataset, A. Kiendler-Scharr for Cabauw AMS data, Eriko Nemitz for the Chilboton data, Karine Sellegri for the Puy de Dôme dataset and Jose-Luis Jimenez for the measurements data in Montseny. The AMS measurements were funded through the European EUCAARI IP. We would like to acknowledge EMEP for the measurement data used here, HEA-PRTLI4, EPA Ireland, and the Science Foundation Ireland for facilitating measurements at Mace Head.

References

Aksoyoglu, S., Keller, J., Barmpadimos, I., Oderbolz, D., Lanz, V. A., Prévôt, A. S. H. and Baltensperger, U.: Aerosol modelling in Europe with a focus on Switzerland during summer and winter episodes, Atmos. Chem. Phys., 11 (14), 7355–7373, doi:10.5194/acp-11-7355-2011, 2011.

Bergström, R., Denier van der Gon, H. A. C., Prévôt, A. S. H., Yttri, K. E. and Simpson, D.: Modelling of organic aerosols over Europe (2002–2007) using a volatility basis set (VBS) framework: application of different assumptions regarding the formation of secondary organic aerosol, Atmos. Chem. Phys., 12 (18), 8499–8527, doi:10.5194/acp-12-8499-2012, 2012.

Bessagnet, B., Colette, A., Meleux, F., Rouïl, L., Ung, A., Favez, O., Cuvelier, C., Thunis, P., Tsyro, S., Stern, R., Manders, A., Kranenburg, R., Aulinger, A., Bieser, J., Mircea, M., Briganti, A., Cappelletti, A., Calori, G., Finardi, S., Silibello, C., Ciarelli, G., Aksoyoglu, S., Prévôt, A., Pay, M. T., Baldasano, J. M., García Vivanco, M., Garrido, J. L., Palomino, I., Martín, F., Pirovano, G., Roberts, P., Gonzalez, L., White, L., Menut, L., Dupont, J. C., Carnevale, C. and Pederzoli, A.: The EURODELTA III exercise – Model evaluation with observations issued from the 2009 EMEP intensive period and standard measurements in Feb/Mar 2009, 2014.

Boylan, J. W. and Russell, A. G.: PM and light extinction model performance metrics, goals, and criteria for three-dimensional air quality models, Atmos. Environ., 40 (26), 4946–4959, doi:10.1016/j.atmosenv.2005.09.087, 2006.

Bruns, E. A., El Haddad, I., Slowik, J. G., Kilic, D., Klein, F., Baltensperger, U. and Prévôt, A. S. H.: Identification of significant precursor gases of secondary organic aerosols from residential wood combustion, Sci. Rep., 6, 27881, doi:10.1038/srep27881, 2016.

Canonaco, F., Crippa, M., Slowik, J. G., Baltensperger, U. and Prévôt, A. S. H.: SoFi, an IGOR-based interface for the efficient use of the generalized multilinear engine (ME-2) for the source apportionment: ME-2 application to aerosol mass spectrometer data, Atmos. Meas. Tech., 6 (12), 3649–3661, doi:10.5194/amt-6-3649-2013, 2013.

Canonaco, F., Slowik, J. G., Baltensperger, U. and Prévôt, A. S. H.: Seasonal differences in oxygenated organic aerosol composition: implications for emissions sources and factor analysis, Atmos. Chem. Phys., 15 (12), 6993–7002, doi:10.5194/acp-15-6993-2015, 2015.

Chang, J. S., Brost, R. A., Isaksen, I. S. A., Madronich, S., Middleton, P., Stockwell, W. R. and Walcek, C. J.: A three-dimensional Eulerian acid deposition model: Physical concepts and formulation, J. Geophys. Res. Atmospheres, 92 (D12), 14681–14700, doi:10.1029/JD092iD12p14681, 1987.

Ciarelli, G., Aksoyoglu, S., Crippa, M., Jimenez, J.-L., Nemitz, E., Sellegri, K., Äijälä, M., Carbone, S., Mohr, C., O';Dowd, C., Poulain, L., Baltensperger, U. and Prévôt, A. S. H.: Evaluation of European air quality modelled by CAMx including the volatility basis set scheme, Atmos. Chem. Phys., 16 (16), 10313–10332, doi:10.5194/acp-16-10313-2016, 2016a.

Ciarelli, G., El Haddad, I., Bruns, E., Aksoyoglu, S., Möhler, O., Baltensperger, U. and Prévôt, A. S. H.: Constraining a hybrid volatility basis set model for aging of wood burning emissions using smog chamber experiments, Geosci. Model Dev. , accepted, 2016b.

Crippa, M., Canonaco, F., Lanz, V. A., Äijälä, M., Allan, J. D., Carbone, S., Capes, G., Ceburnis, D., Dall'Osto, M., Day, D. A., DeCarlo, P. F., Ehn, M., Eriksson, A., Freney, E., Hildebrandt Ruiz, L., Hillamo, R., Jimenez, J. L., Junninen, H., Kiendler-Scharr, A., Kortelainen, A.-M., Kulmala, M., Laaksonen, A., Mensah, A. A., Mohr, C., Nemitz, E., O'Dowd, C., Ovadnevaite, J., Pandis, S. N., Petäjä, T., Poulain, L., Saarikoski, S., Sellegri, K., Swietlicki, E., Tiitta, P., Worsnop, D. R., Baltensperger, U. and Prévôt, A. S. H.: Organic aerosol components derived from 25 AMS data sets across Europe using a consistent ME-2 based source apportionment approach, Atmos. Chem. Phys., 14 (12), 6159–6176, doi:10.5194/acp-14-6159-2014, 2014.

Cubison, M. J., Ortega, A. M., Hayes, P. L., Farmer, D. K., Day, D., Lechner, M. J., Brune, W. H., Apel, E., Diskin, G. S., Fisher, J. A., Fuelberg, H. E., Hecobian, A., Knapp, D. J., Mikoviny, T., Riemer, D., Sachse, G. W., Sessions, W., Weber, R. J., Weinheimer, A. J., Wisthaler, A. and Jimenez, J. L.: Effects of aging on organic aerosol from open biomass burning smoke in aircraft and laboratory studies, Atmos. Chem. Phys., 11 (23), 12049–12064, doi:10.5194/acp-11-12049-2011, 2011.

Denier van der Gon, H. A. C., Bergström, R., Fountoukis, C., Johansson, C., Pandis, S. N., Simpson, D. and Visschedijk, A. J. H.: Particulate emissions from residential wood

544 combustion in Europe – revised estimates and an evaluation, Atmos. Chem. Phys., 15 (11),
545 6503–6519, doi:10.5194/acp-15-6503-2015, 2015.

546 Donahue, N. M., Epstein, S. A., Pandis, S. N. and Robinson, A. L.: A two-dimensional
547 volatility basis set: 1. organic-aerosol mixing thermodynamics, Atmos. Chem. Phys., 11 (7),
548 3303–3318, doi:10.5194/acp-11-3303-2011, 2011.

549 Donahue, N. M., Chuang, W., Epstein, S. A., Kroll, J. H., Worsnop, D. R., Robinson, A. L.,
550 Adams, P. J. and Pandis, S. N.: Why do organic aerosols exist? Understanding aerosol
551 lifetimes using the two-dimensional volatility basis set, Environ. Chem., 10 (3), 151,
552 doi:10.1071/EN13022, 2013.

553 ENVIRON: User's Guide, Comprehensive Air Quality Model with Extensions (CAMx),
554 Version 5.40, Environ International Corporation, California, 2011.

555 Fountoukis, C., Megaritis, A. G., Skyllakou, K., Charalampidis, P. E., Pilinis, C., Denier van
556 der Gon, H. A. C., Crippa, M., Canonaco, F., Mohr, C., Prévôt, A. S. H., Allan, J. D., Poulain,
557 L., Petäjä, T., Tiitta, P., Carbone, S., Kiendler-Scharr, A., Nemitz, E., O'Dowd, C., Swietlicki,
558 E. and Pandis, S. N.: Organic aerosol concentration and composition over Europe: insights
559 from comparison of regional model predictions with aerosol mass spectrometer factor
560 analysis, Atmos. Chem. Phys., 14 (17), 9061–9076, doi:10.5194/acp-14-9061-2014, 2014.

561 Grieshop, A. P., Logue, J. M., Donahue, N. M. and Robinson, A. L.: Laboratory investigation
562 of photochemical oxidation of organic aerosol from wood fires 1: measurement and
563 simulation of organic aerosol evolution, Atmos. Chem. Phys., 9 (4), 1263–1277,
564 doi:10.5194/acp-9-1263-2009, 2009.

565 Guenther, A. B., Jiang, X., Heald, C. L., Sakulyanontvittaya, T., Duhl, T., Emmons, L. K. and
566 Wang, X.: The Model of Emissions of Gases and Aerosols from Nature version 2.1
567 (MEGAN2.1): an extended and updated framework for modeling biogenic emissions, Geosci.
568 Model Dev., 5 (6), 1471–1492, doi:10.5194/gmd-5-1471-2012, 2012.

569 Hallquist, M., Wenger, J. C., Baltensperger, U., Rudich, Y., Simpson, D., Claeys, M.,
570 Dommen, J., Donahue, N. M., George, C., Goldstein, A. H., Hamilton, J. F., Herrmann, H.,
571 Hoffmann, T., Iinuma, Y., Jang, M., Jenkin, M. E., Jimenez, J. L., Kiendler-Scharr, A.,
572 Maenhaut, W., McFiggans, G., Mentel, T. F., Monod, A., Prévôt, A. S. H., Seinfeld, J. H.,
573 Surratt, J. D., Szmigielski, R. and Wildt, J.: The formation, properties and impact of

574 secondary organic aerosol: current and emerging issues, Atmos. Chem. Phys., 9 (14), 5155–
575 5236, doi:10.5194/acp-9-5155-2009, 2009.

576 Heald, C. L., Kroll, J. H., Jimenez, J. L., Docherty, K. S., DeCarlo, P. F., Aiken, A. C., Chen,
577 Q., Martin, S. T., Farmer, D. K. and Artaxo, P.: A simplified description of the evolution of
578 organic aerosol composition in the atmosphere, Geophys. Res. Lett., 37 (8), n/a-n/a,
579 doi:10.1029/2010GL042737, 2010.

580 Hodzic, A., Kasibhatla, P. S., Jo, D. S., Cappa, C. D., Jimenez, J. L., Madronich, S., and Park,
581 R. J.: Rethinking the global secondary organic aerosol (SOA) budget: stronger production,
582 faster removal, shorter lifetime, Atmos. Chem. Phys., 16, 7917-7941, doi:10.5194/acp-16-
583 7917-2016, 2016.

584 Huang, R.-J., Zhang, Y., Bozzetti, C., Ho, K.-F., Cao, J.-J., Han, Y., Daellenbach, K. R.,
585 Slowik, J. G., Platt, S. M., Canonaco, F., Zotter, P., Wolf, R., Pieber, S. M., Bruns, E. A.,
586 Crippa, M., Ciarelli, G., Piazzalunga, A., Schwikowski, M., Abbaszade, G., Schnelle-Kreis,
587 J., Zimmermann, R., An, Z., Szidat, S., Baltensperger, U., Haddad, I. E. and Prévôt, A. S. H.:
588 High secondary aerosol contribution to particulate pollution during haze events in China,
589 Nature, 514 (7521), 218–222, doi:10.1038/nature13774, 2014.

590 Jimenez, J. L., Canagaratna, M. R., Donahue, N. M., Prevot, A. S. H., Zhang, Q., Kroll, J. H.,
591 DeCarlo, P. F., Allan, J. D., Coe, H., Ng, N. L., Aiken, A. C., Docherty, K. S., Ulbrich, I. M.,
592 Grieshop, A. P., Robinson, A. L., Duplissy, J., Smith, J. D., Wilson, K. R., Lanz, V. A.,
593 Hueglin, C., Sun, Y. L., Tian, J., Laaksonen, A., Raatikainen, T., Rautiainen, J., Vaattovaara,
594 P., Ehn, M., Kulmala, M., Tomlinson, J. M., Collins, D. R., Cubison, M. J., Dunlea, E. J.,
595 Huffman, J. A., Onasch, T. B., Alfarra, M. R., Williams, P. I., Bower, K., Kondo, Y.,
596 Schneider, J., Drewnick, F., Borrmann, S., Weimer, S., Demerjian, K., Salcedo, D., Cottrell,
597 L., Griffin, R., Takami, A., Miyoshi, T., Hatakeyama, S., Shimono, A., Sun, J. Y., Zhang, Y.
598 M., Dzepina, K., Kimmel, J. R., Sueper, D., Jayne, J. T., Herndon, S. C., Trimborn, A. M.,
599 Williams, L. R., Wood, E. C., Middlebrook, A. M., Kolb, C. E., Baltensperger, U. and
600 Worsnop, D. R.: Evolution of organic aerosols in the atmosphere, Science, 326 (5959), 1525–
601 1529, doi:10.1126/science.1180353, 2009.

602 Jolleys, M. D., Coe, H., McFiggans, G., Capes, G., Allan, J. D., Crosier, J., Williams, P. I.,
603 Allen, G., Bower, K. N., Jimenez, J. L., Russell, L. M., Grutter, M. and Baumgardner, D.:

Characterizing the Aging of Biomass Burning Organic Aerosol by Use of Mixing Ratios: A Meta-analysis of Four Regions, Environ. Sci. Technol., 46 (24), 13093–13102, doi:10.1021/es302386v, 2012.

Koo, B., Knipping, E. and Yarwood, G.: 1.5-Dimensional volatility basis set approach for modeling organic aerosol in CAMx and CMAQ, Atmos. Environ., 95, 158–164, doi:10.1016/j.atmosenv.2014.06.031, 2014.

Kuenen, J. J. P., Visschedijk, A. J. H., Jozwicka, M. and Denier van der Gon, H. A. C.: TNO-MACC_II emission inventory; a multi-year (2003–2009) consistent high-resolution European emission inventory for air quality modelling, Atmos. Chem. Phys., 14 (20), 10963–10976, doi:10.5194/acp-14-10963-2014, 2014.

Kulmala, M., Asmi, A., Lappalainen, H. K., Baltensperger, U., Brenguier, J.-L., Facchini, M. C., Hansson, H.-C., Hov, Ø., O'Dowd, C. D., Pöschl, U., Wiedensohler, A., Boers, R., Boucher, O., de Leeuw, G., Denier van der Gon, H. A. C., Feichter, J., Krejci, R., Laj, P., Lihavainen, H., Lohmann, U., McFiggans, G., Mentel, T., Pilinis, C., Riipinen, I., Schulz, M., Stohl, A., Swietlicki, E., Vignati, E., Alves, C., Amann, M., Ammann, M., Arabas, S., Artaxo, P., Baars, H., Beddows, D. C. S., Bergström, R., Beukes, J. P., Bilde, M., Burkhart, J. F., Canonaco, F., Clegg, S. L., Coe, H., Crumeyrolle, S., D'Anna, B., Decesari, S., Gilardoni, S., Fischer, M., Fjaeraa, A. M., Fountoukis, C., George, C., Gomes, L., Halloran, P., Hamburger, T., Harrison, R. M., Herrmann, H., Hoffmann, T., Hoose, C., Hu, M., Hyvärinen, A., Hõrrak, U., Iinuma, Y., Iversen, T., Josipovic, M., Kanakidou, M., Kiendler-Scharr, A., Kirkevåg, A., Kiss, G., Klimont, Z., Kolmonen, P., Komppula, M., Kristjánsson, J.-E., Laakso, L., Laaksonen, A., Labonnote, L., Lanz, V. A., Lehtinen, K. E. J., Rizzo, L. V., Makkonen, R., Manninen, H. E., McMeeking, G., Merikanto, J., Minikin, A., Mirme, S., Morgan, W. T., Nemitz, E., O'Donnell, D., Panwar, T. S., Pawlowska, H., Petzold, A., Pienaar, J. J., Pio, C., Plass-Duelmer, C., Prévôt, A. S. H., Pryor, S., Reddington, C. L., Roberts, G., Rosenfeld, D., Schwarz, J., Seland, Ø., et al.: General overview: European Integrated project on Aerosol Cloud Climate and Air Quality interactions (EUCAARI) – integrating aerosol research from nano to global scales, Atmos. Chem. Phys., 11, 13061–13143, doi:10.5194/acp-11-13061-2011, 2011.

633 Lipsky, E. M. and Robinson, A. L.: Effects of Dilution on Fine Particle Mass and Partitioning
634 of Semivolatile Organics in Diesel Exhaust and Wood Smoke, Environ. Sci. Technol., 40 (1),
635 155–162, doi:10.1021/es050319p, 2006.

636 May, A. A., Levin, E. J. T., Hennigan, C. J., Riipinen, I., Lee, T., Collett, J. L., Jimenez, J. L.,
637 Kreidenweis, S. M. and Robinson, A. L.: Gas-particle partitioning of primary organic aerosol
638 emissions: 3. Biomass burning, J. Geophys. Res. Atmospheres, 118 (19), 2013JD020286,
639 doi:10.1002/jgrd.50828, 2013.

640 Nenes, A., Pandis, S. N. and Pilinis, C.: ISORROPIA: a new thermodynamic equilibrium
641 model for multiphase multicomponent inorganic aerosols, Aquat. Geochem., 4, 123–152,
642 1998, Aquat. Geochem., 4, 123–152, 1998.

643 Ots, R., Young, D. E., Vieno, M., Xu, L., Dunmore, R. E., Allan, J. D., Coe, H., Williams, L.
644 R., Herndon, S. C., Ng, N. L., Hamilton, J. F., Bergström, R., Di Marco, C., Nemitz, E.,
645 Mackenzie, I. A., Kuenen, J. J. P., Green, D. C., Reis, S. and Heal, M. R.: Simulating
646 secondary organic aerosol from missing diesel-related intermediate-volatility organic
647 compound emissions during the Clean Air for London (ClearfLo) campaign, Atmos. Chem.
648 Phys., 16 (10), 6453–6473, doi:10.5194/acp-16-6453-2016, 2016.

649 Paatero, P.: The Multilinear Engine: A Table-Driven, Least Squares Program for Solving
650 Multilinear Problems, including the n-Way Parallel Factor Analysis Model, J. Comput.
651 Graph. Stat., 8 (4), 854, doi:10.2307/1390831, 1999.

652 Robinson, A. L., Donahue, N. M., Shrivastava, M. K., Weitkamp, E. A., Sage, A. M.,
653 Grieshop, A. P., Lane, T. E., Pierce, J. R. and Pandis, S. N.: Rethinking Organic Aerosols:
654 Semivolatile Emissions and Photochemical Aging, Science, 315 (5816), 1259–1262,
655 doi:10.1126/science.1133061, 2007.

656 Shrivastava, M., Fast, J., Easter, R., Gustafson Jr., W. I., Zaveri, R. A., Jimenez, J. L., Saide,
657 P. and Hodzic, A.: Modeling organic aerosols in a megacity: comparison of simple and
658 complex representations of the volatility basis set approach, Atmos. Chem. Phys., 11, 6639–
659 6662, 2011.

660 Tsigaridis, K., Daskalakis, N., Kanakidou, M., Adams, P. J., Artaxo, P., Bahadur, R.,
661 Balkanski, Y., Bauer, S. E., Bellouin, N., Benedetti, A., Bergman, T., Berntsen, T. K.,
662 Beukes, J. P., Bian, H., Carslaw, K. S., Chin, M., Curci, G., Diehl, T., Easter, R. C., Ghan, S.

J., Gong, S. L., Hodzic, A., Hoyle, C. R., Iversen, T., Jathar, S., Jimenez, J. L., Kaiser, J. W., Kirkevåg, A., Koch, D., Kokkola, H., Lee, Y. H., Lin, G., Liu, X., Luo, G., Ma, X., Mann, G. W., Mihalopoulos, N., Morcrette, J.-J., Müller, J.-F., Myhre, G., Myriokefalitakis, S., Ng, N. L., O'Donnell, D., Penner, J. E., Pozzoli, L., Pringle, K. J., Russell, L. M., Schulz, M., Sciare, J., Seland, Ø., Shindell, D. T., Sillman, S., Skeie, R. B., Spracklen, D., Stavrakou, T., Steenrod, S. D., Takemura, T., Tiitta, P., Tilmes, S., Tost, H., van Noije, T., van Zyl, P. G., von Salzen, K., Yu, F., Wang, Z., Wang, Z., Zaveri, R. A., Zhang, H., Zhang, K., Zhang, Q. and Zhang, X.: The AeroCom evaluation and intercomparison of organic aerosol in global models, Atmos. Chem. Phys., 14 (19), 10845–10895, doi:10.5194/acp-14-10845-2014, 2014.

Tsimpidi, A. P., Karydis, V. A., Zavala, M., Lei, W., Molina, L., Ulbrich, I. M., Jimenez, J. L. and Pandis, S. N.: Evaluation of the volatility basis-set approach for the simulation of organic aerosol formation in the Mexico City metropolitan area, Atmos. Chem. Phys., 10, 525–546, 2010.

Vaughan, A. R., Lee, J. D., Misztal, P. K., Metzger, S., Shaw, M. D., Lewis, A. C., Purvis, R. M., Carslaw, D. C., Goldstein, A. H., Hewitt, C. N., Davison, B., Beevers, S. D. and Karl, T. G.: Spatially resolved flux measurements of NO_x from London suggest significantly higher emissions than predicted by inventories, Faraday Discuss, doi:10.1039/C5FD00170F, 2016.

Woody, M. C., Baker, K. R., Hayes, P. L., Jimenez, J. L., Koo, B. and Pye, H. O. T.: Understanding sources of organic aerosol during CalNex-2010 using the CMAQ-VBS, Atmos. Chem. Phys., 16 (6), 4081–4100, doi:10.5194/acp-16-4081-2016, 2016.

Yarwood, G.: Updates to the Carbon Bond Chemical 852 Mechanism: CB05, 2005.

Young, D. E., Allan, J. D., Williams, P. I., Green, D. C., Flynn, M. J., Harrison, R. M., Yin, J., Gallagher, M. W. and Coe, H.: Investigating the annual behaviour of submicron secondary inorganic and organic aerosols in London, Atmos. Chem. Phys., 15 (11), 6351–6366, doi:10.5194/acp-15-6351-2015, 2015.

4 Tables and Figures

Table 1. Properties of the VBS space. Oxygen numbers for each volatility bin were calculated using the group-contribution of Donahue et al. (2011). Hydrogen numbers were calculated from the van Krevelen relation (Heald et al., 2010).

	log (C*)	Oxygen number	Carbon number	Hydrogen number	Molecular weight
POA set1* (BBOA-like) Primary biomass burning (BBPOA)	-1	4.11	11.00	17.89	216
	0	3.43	11.75	20.07	216
	1	2.73	12.50	22.27	216
	2	2.01	13.25	24.49	216
	3	1.27	14.00	26.73	215
SOA set2* (BBOA-like) SOA from SVOCs biomass burning	-1	4.53	9.00	13.47	194
	0	4.00	9.25	14.50	189
	1	3.40	9.50	15.60	184
	2	2.83	9.75	16.67	179
SOA set3* (BBOA-like) SOA from VOC/IVOCs biomass burning and biogenics	-1	5.25	5.00	4.75	149
	0	4.70	5.25	5.80	144
	1	4.20	5.50	6.80	140
	2	3.65	5.75	7.85	135
	3	3.15	6.00	8.85	131
POA set1** (HOA-like) Rest of primary anthropogenic sources	-1	2.69	17.00	31.3	278
	0	2.02	17.50	33.0	275
	1	1.34	18.00	34.7	272
	2	0.63	18.50	36.4	268
	3	0.0	19.00	38.0	266
SOA set1** (HOA-like) SOA from rest of all	-1	4.90	7.00	9.10	172
	0	4.38	7.25	10.1	167
	1	3.84	7.50	11.2	163

anthropogenic in all volatility range (SVOCs,IVOCs,VOCs)	2	3.30	7.75	12.2	158
	3	2.74	8.00	13.3	153

694

695 **Based on Ciarelli et al. (2016b).*

696 ***Molecular structure as in Koo et al. (2014) and Ciarelli et al. (2016a).*

697

698 Table 2. Statistics of OA for the VBS_BC_NEW case for February-March 2009 at each AMS
699 site as well as an average of all sites for both VBS_BC_NEW and VBS_BC. Bold numbers
700 represent the stations were model performance criteria were met.

Site*	Mean observed OA ($\mu g\ m^{-3}$)	Mean modelled OA ($\mu g\ m^{-3}$)	MB ($\mu g\ m^{-3}$)	ME ($\mu g\ m^{-3}$)	MFB [-]	MFE [-]	r	R^2
Barcelona (BCN)	8.3	5.1	-3.1	3.7	**-0.4**	**0.5**	0.6	0.4
Cabauw (CBW)	1.2	1.5	0.3	0.7	**0.1**	**0.5**	0.7	0.4
Chilbolton (CHL)	2.4	1.0	-1.4	1.5	-0.9	0.9	0.8	0.6
Helsinki (HEL)	2.7	3.6	0.9	1.8	**0.3**	**0.6**	0.3	0.1
Hyytiälä (SMR)	1.3	1.7	0.3	0.8	**-0.1**	**0.6**	0.8	0.6
Mace Head (MHD)	0.8	0.7	-0.1	0.3	**-0.1**	**0.7**	0.7	0.5
Melpitz (MPZ)	1.5	0.8	-0.6	0.9	-0.6	0.7	0.6	0.3
Montseny (MSY)	3.1	3.5	0.4	2.0	**0.1**	**0.6**	0.4	0.1
Payerne (PAY)	4.1	2.9	-1.2	1.9	**-0.5**	**0.7**	0.7	0.4
Puy de Dôme (PDD)	0.6	1.1	0.4	0.8	0.3	0.8	0.4	0.2
Vavihill (VAV)	3.9	2.1	-1.8	2.0	-0.8	0.8	0.8	0.6
VBS_BC_NEW	3.0	2.3	-0.7	1.6	**-0.3**	**0.7**	0.8	0.6
VBS_BC	3.0	1.4	-1.5	1.8	-0.6	0.8	0.8	0.6

(Ciarelli et al., 2016a)

* Model OA concentrations extracted at surface level except for the stations of Puy de Dôme and Montseny.

Table 3. Statistics of POA for the VBS_BC_NEW case for February-March 2009 at each AMS site as well as an average of all sites for both VBS_BC_NEW and VBS_BC. Bold numbers represent the stations were model performance criteria were met.

Site	Mean observed POA ($\mu g\ m^{-3}$)	Mean modelled POA ($\mu g\ m^{-3}$)	MB ($\mu g\ m^{-3}$)	ME ($\mu g\ m^{-3}$)	MFB [-]	MFE [-]	r	R^2
Barcelona	4.0	2.0	-2.1	2.4	**-0.5**	**0.7**	0.4	0.2
Cabauw	0.4	0.9	0.5	0.5	0.8	0.9	0.5	0.2
Chilbolton	1.0	0.5	-0.5	0.5	**-0.6**	**0.7**	0.8	0.6
Helsinki	0.8	2.5	1.7	1.7	1.0	1.0	0.2	0.0
Hyytiälä	0.1	0.5	0.4	0.4	1.3	1.3	0.5	0.3
Mace Head	0.2	0.1	-0.1	0.2	0.5	1.0	0.2	0.1
Melpitz	0.3	0.3	0.1	0.2	**0.3**	**0.7**	0.5	0.2
Montseny	0.5	0.4	0.0	0.3	**0.2**	**0.7**	0.3	0.1
Payerne	0.7	1.1	0.3	0.6	**0.5**	**0.7**	0.5	0.3
Puy de Dôme	0.2	0.3	0.1	0.2	0.5	0.9	0.2	0.1
Vavihill	1.1	1.0	-0.1	0.6	**-0.3**	**0.7**	0.5	0.2
VBS_BC_NEW	0.9	0.9	-0.1	0.7	0.3	0.8	0.6	0.3
VBS_BC (Ciarelli et al., 2016a)	0.9	0.9	0.0	0.8	0.3	0.8	0.6	0.4

Table 4. Statistics of SOA for the VBS_BC_NEW case for February-March 2009 at each AMS site as well as an average of all sites for both VBS_BC_NEW and VBS_BC. Bold number represents the stations were model performance criteria were met.

Site	Mean observed SOA ($\mu g\ m^{-3}$)	Mean modelled SOA ($\mu g\ m^{-3}$)	MB ($\mu g\ m^{-3}$)	ME ($\mu g\ m^{-3}$)	MFB [-]	MFE [-]	r	R^2
Barcelona	4.4	3.2	-1.2	1.6	**-0.4**	**0.5**	0.7	0.5
Cabauw	1.0	0.6	-0.4	0.6	-0.7	0.9	0.7	0.4
Chilbolton	1.4	0.5	-0.9	1.0	-1.1	1.2	0.7	0.5
Helsinki	1.8	1.1	-0.7	1.1	-0.7	0.9	0.4	0.2
Hyytiälä	1.2	1.1	-0.1	0.7	-0.7	1.0	0.8	0.6
Mace Head	0.4	0.5	0.2	0.6	0.3	1.0	0.4	0.2
Melpitz	1.2	0.5	-0.7	0.8	-1.0	1.1	0.6	0.4
Montseny	2.6	3.1	0.5	1.8	**0.0**	**0.7**	0.4	0.1
Payerne	3.7	2.0	-1.7	2.1	-0.8	0.9	0.5	0.3
Puy de Dôme	0.6	0.9	0.3	0.8	0.2	0.9	0.2	0.1
Vavihill	2.8	1.1	-1.7	1.7	-1.2	1.2	0.8	0.7
VBS_BC_NEW	2.1	1.4	-0.6	1.2	-0.6	0.9	0.7	0.5
VBS_BC (Ciarelli et al., 2016a)	2.1	0.5	-1.5	1.6	-1.1	1.3	0.7	0.6

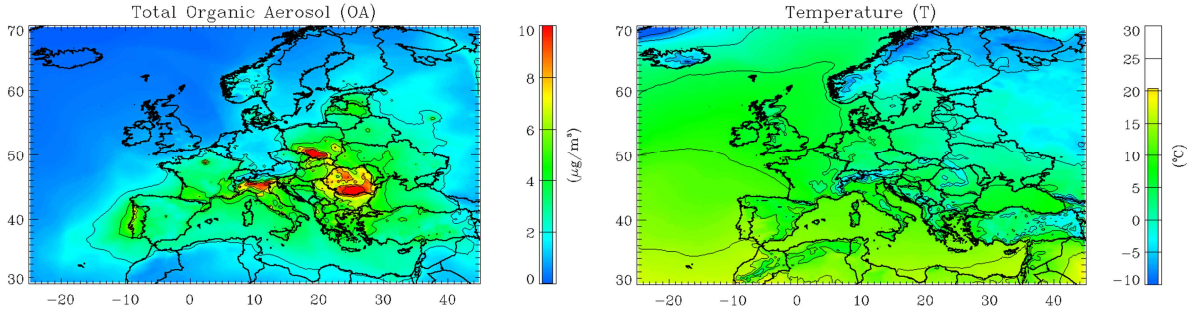

721

722 Figure 1. Modelled average total organic aerosol (OA) concentrations (VBC_BC_NEW) and
723 surface temperature (T) for the period between 25 February and 26 March 2009.

724

725

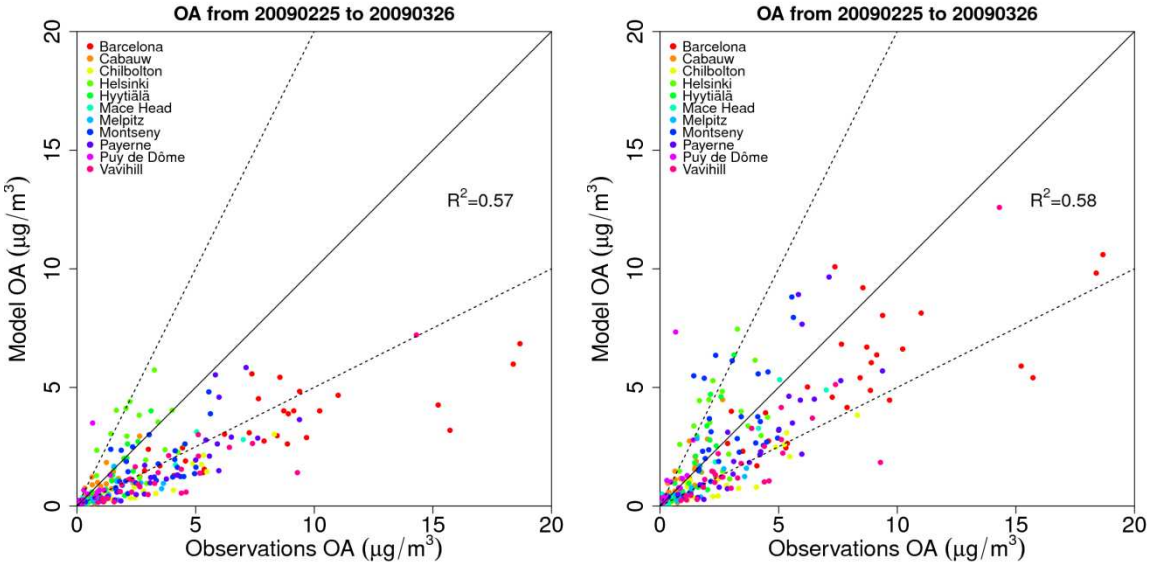

726

727 Figure 2. Daily average scatter plots for OA concentrations at 11 AMS sites for the period
728 between 25 February and 26 March 2009 for VBS_BC (left) and VBS_BC_NEW case (right).
729 Solid lines indicate the 1:1 line. Dotted lines are the 1:2 and 2:1 lines.

730

731

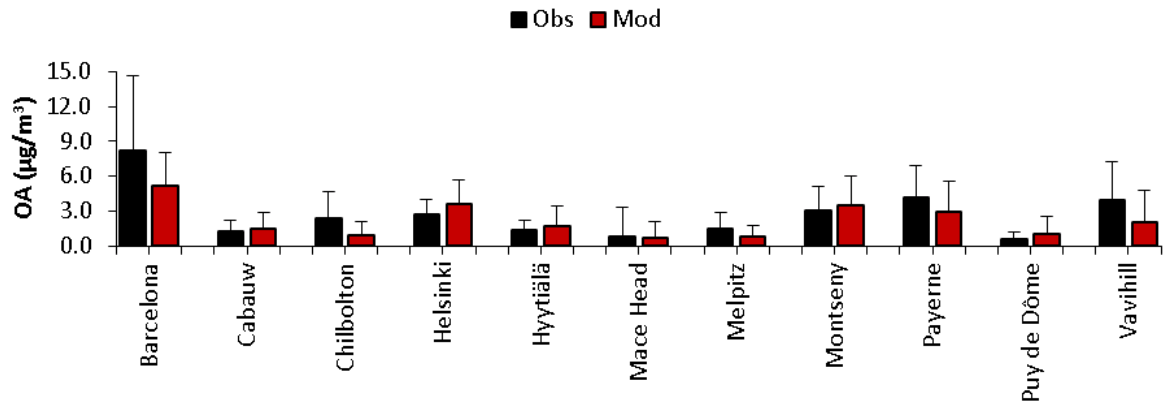

732

733 Figure 3. Observed (black) and modelled (VBS_BC_NEW) (red) average OA mass at AMS
734 sites for the period between 25 February and 26 March 2009.

735

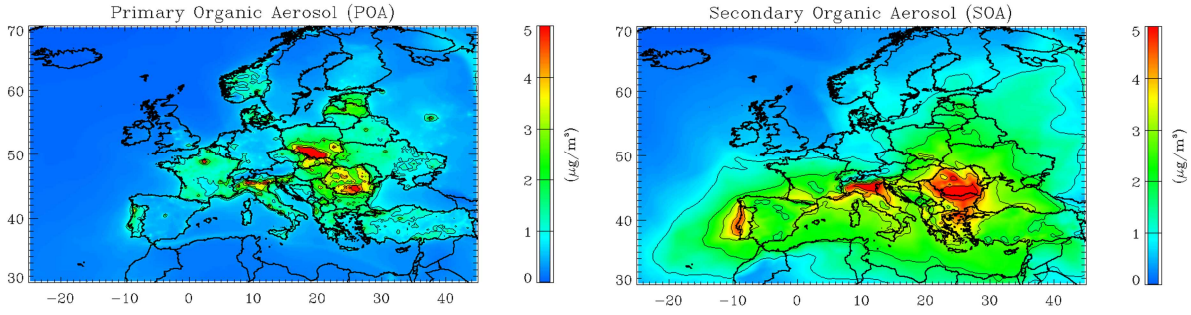

736

737 Figure 4. Modelled average POA (left) and SOA (right) concentrations for the period between
738 25 February and 26 March 2009.

739

740

741

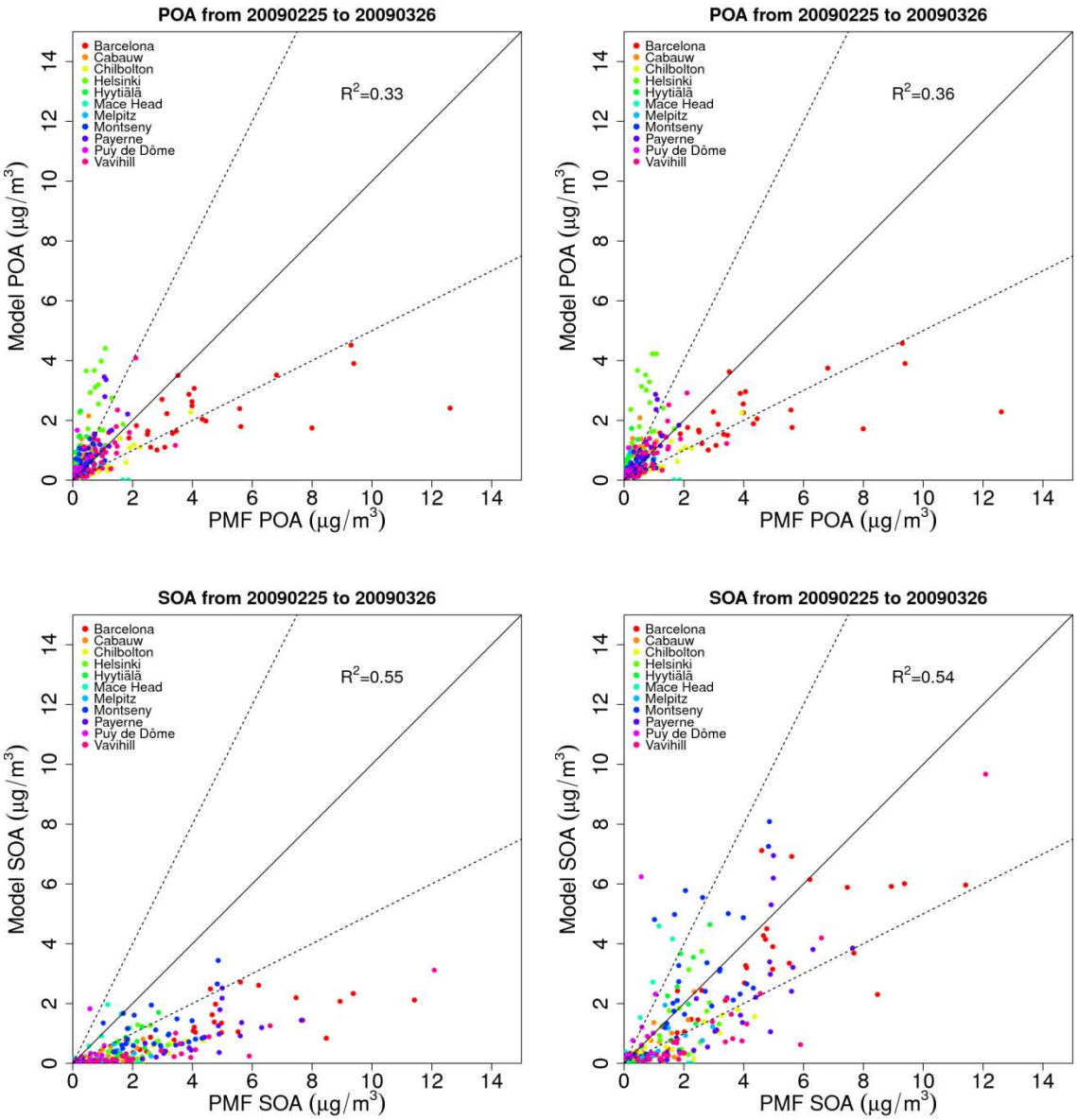

Figure 5. Daily average scatter plots of POA and SOA concentrations at 11 AMS sites for February-March 2009 in VBS_BC (Ciarelli et al., 2016a) (left) and VBS_BC_NEW (right). Solid lines indicate the 1:1 line. Dotted lines are the 1:2 and 2:1 lines.

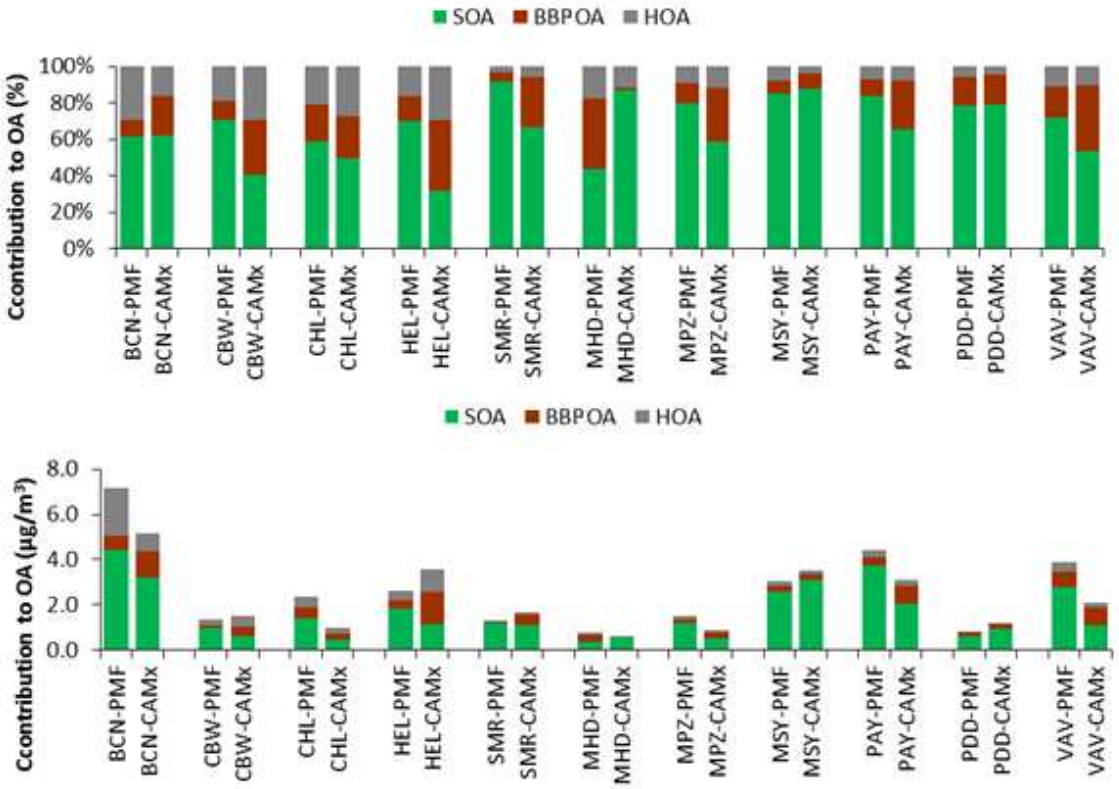

747

748 Figure 6. Relative (upper panel) and absolute (lower panel) contribution of HOA, BBPOA and
749 SOA to OA concentrations at 11 sites from PMF analysis of AMS measurements (first bar)
750 and CAMx VBS_BC_NEW results (second bar) for the period between 25 February and 26
751 March 2009.

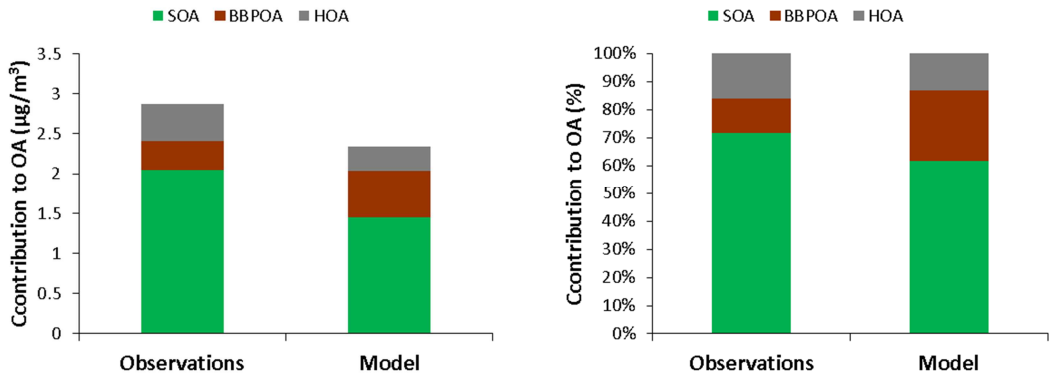

752

753 Figure 7. Measured and modelled average absolute (left panel) and relative (right panel)
754 contributions of HOA, BBPOA and SOA to OA concentrations for all the 11 sites for the
755 period between 25 February and 26 March 2009.

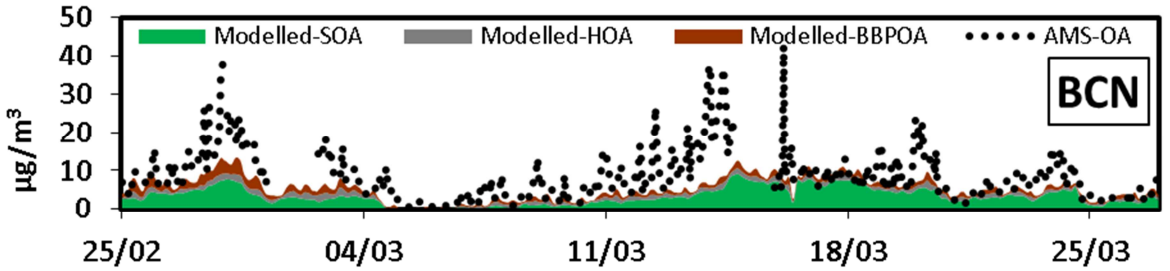

756

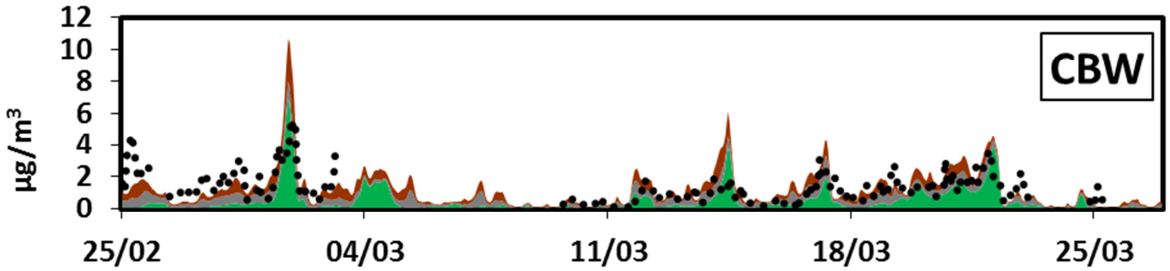

757

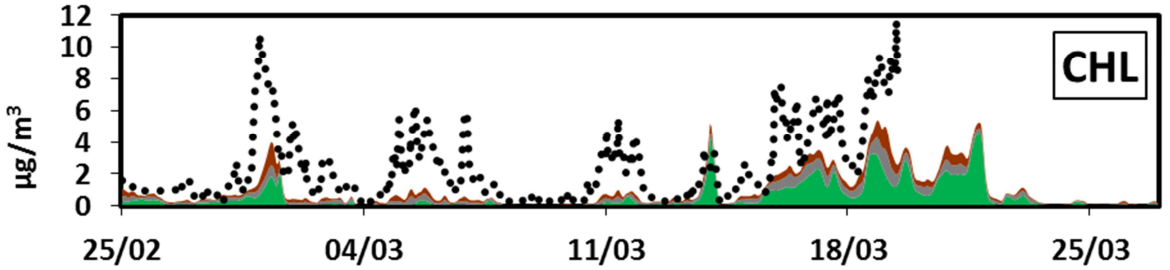

758

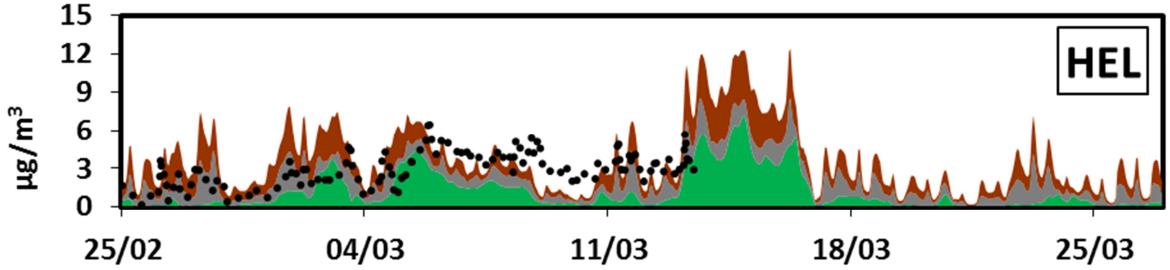

759

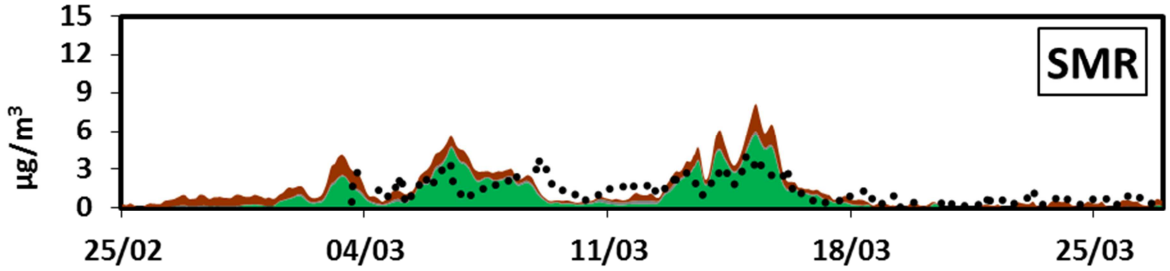

760

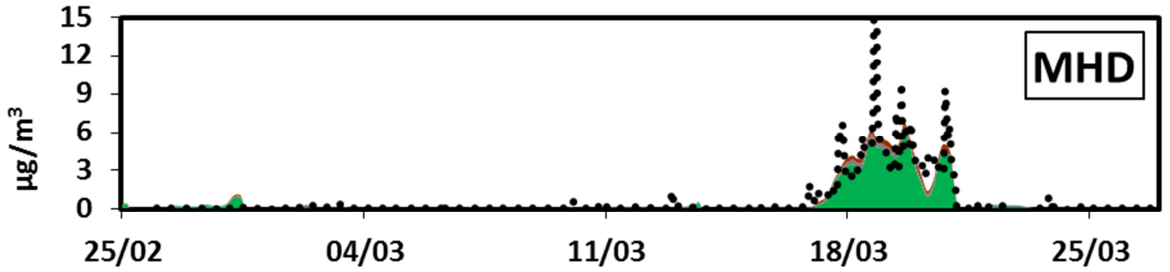

761

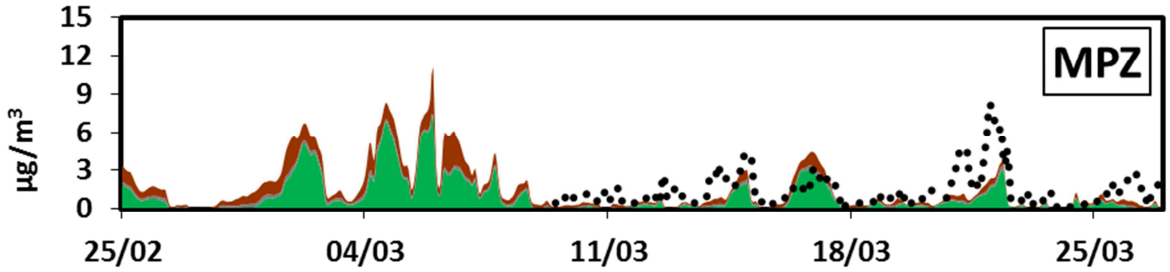

762

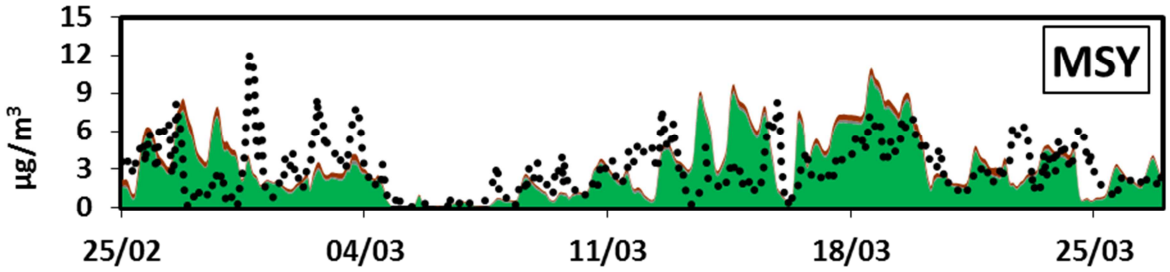

763

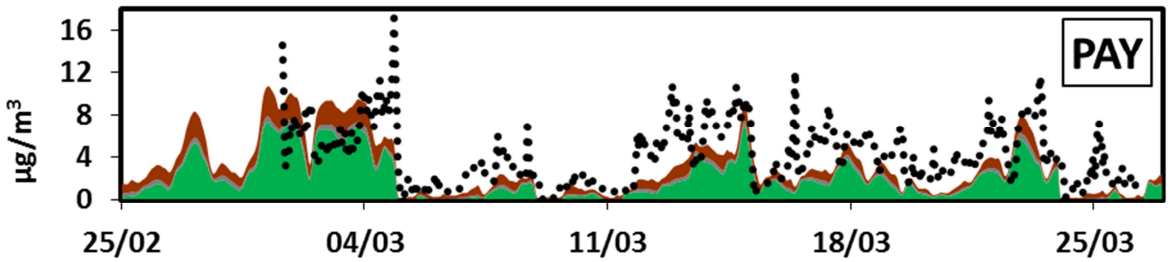

764

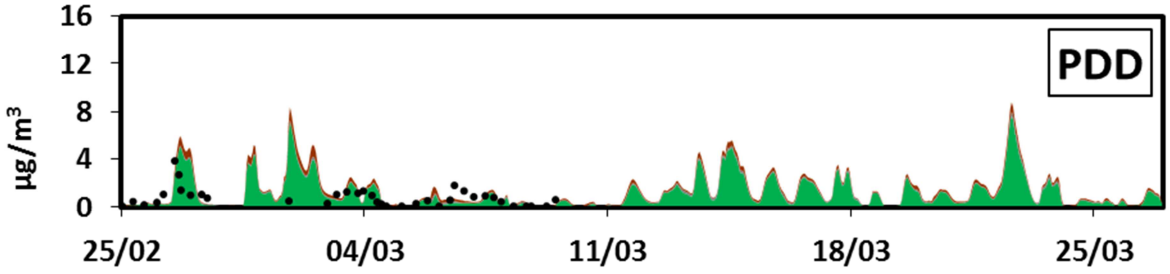

765

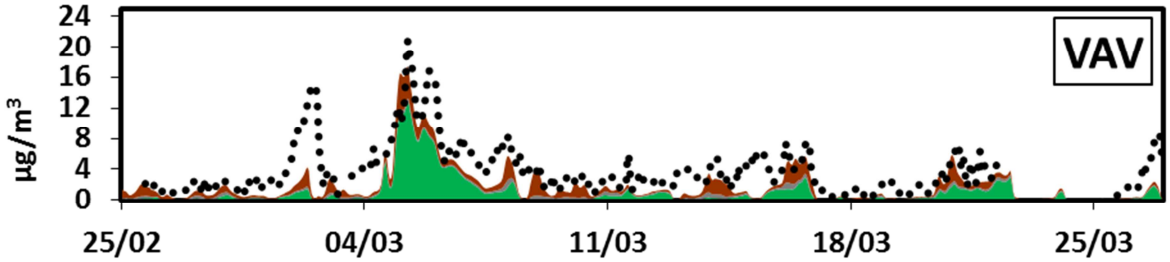

766

767 Figure 8. Comparison of measured hourly OA mass concentrations (AMS-OA dotted line),
768 with modelled components HOA, BBPOA and SOA.

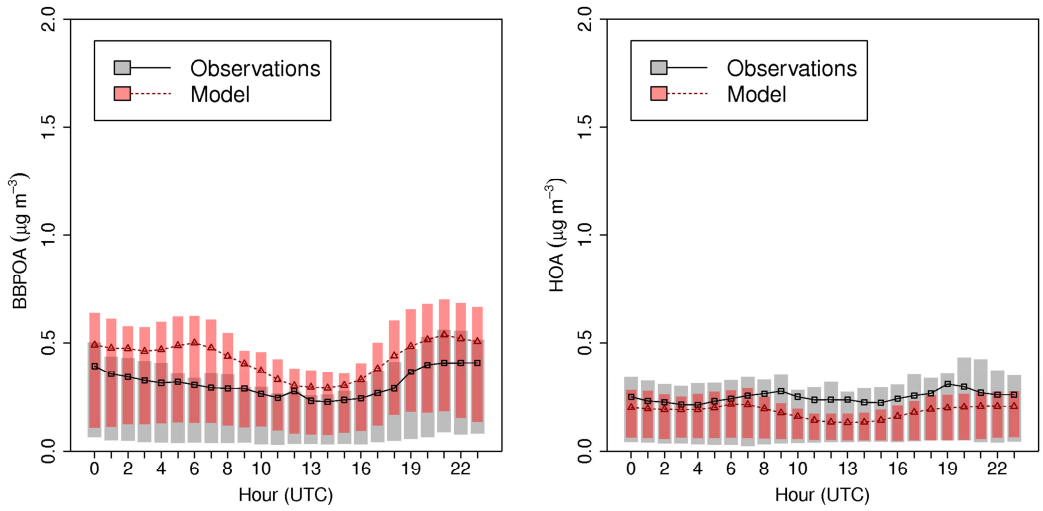

769

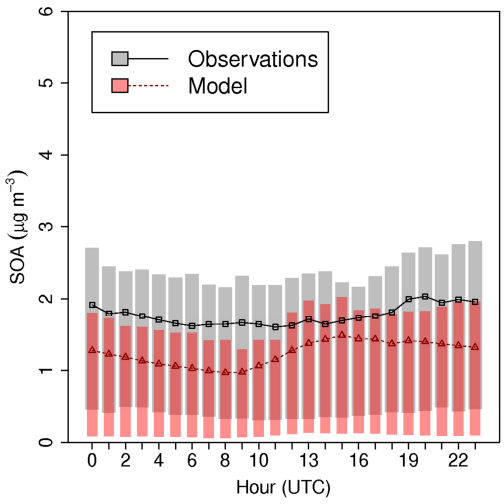

770

771 Figure 9. Comparison of modelled (red) and measured (grey) BBPOA, HOA and SOA diurnal
772 profiles at the rural-background sites. The extent of the bars indicates the 25th and 75th
773 percentiles.

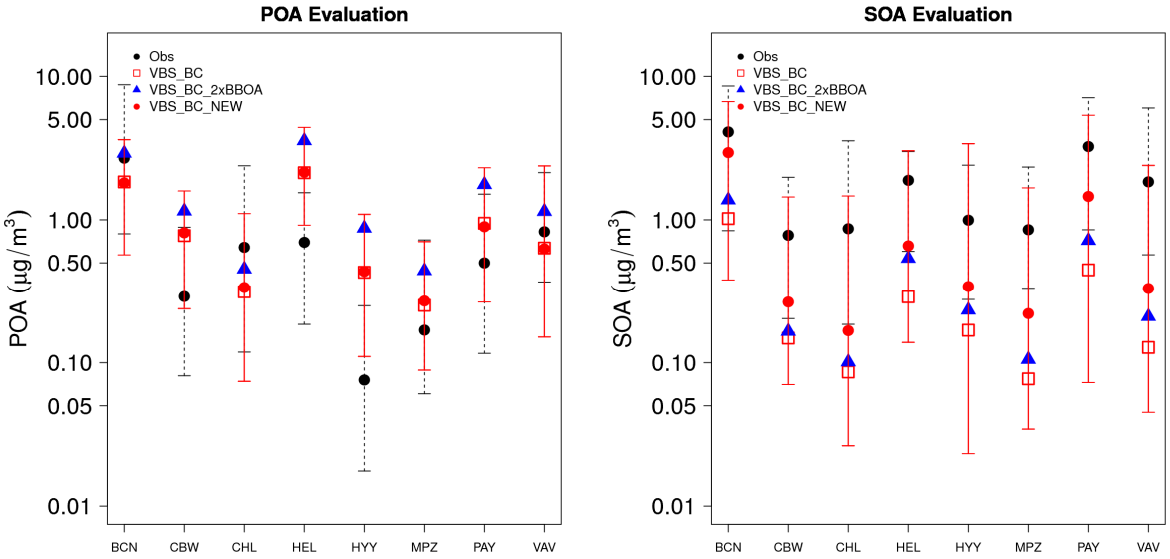

Figure 10. POA (left) and SOA (right) median concentrations at 8 AMS sites for February-March 2009 in the VBS_BC, VBS_BC_2xBBOA and VBS_BC_NEW cases. Dotted lines indicate the 10th and 90th quartile range (also reported in red for the VBS_BC_NEW case). Data for the Puy de Dôme and Montseny sites at higher layers are not available for the VBS_BC_2xBBOA scenario.

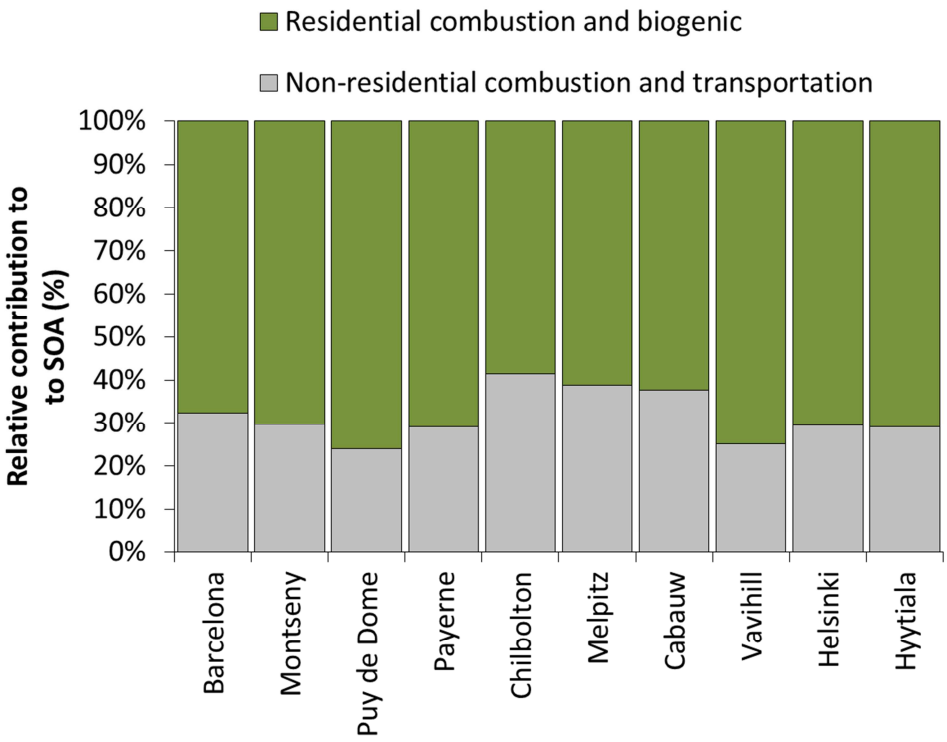

783

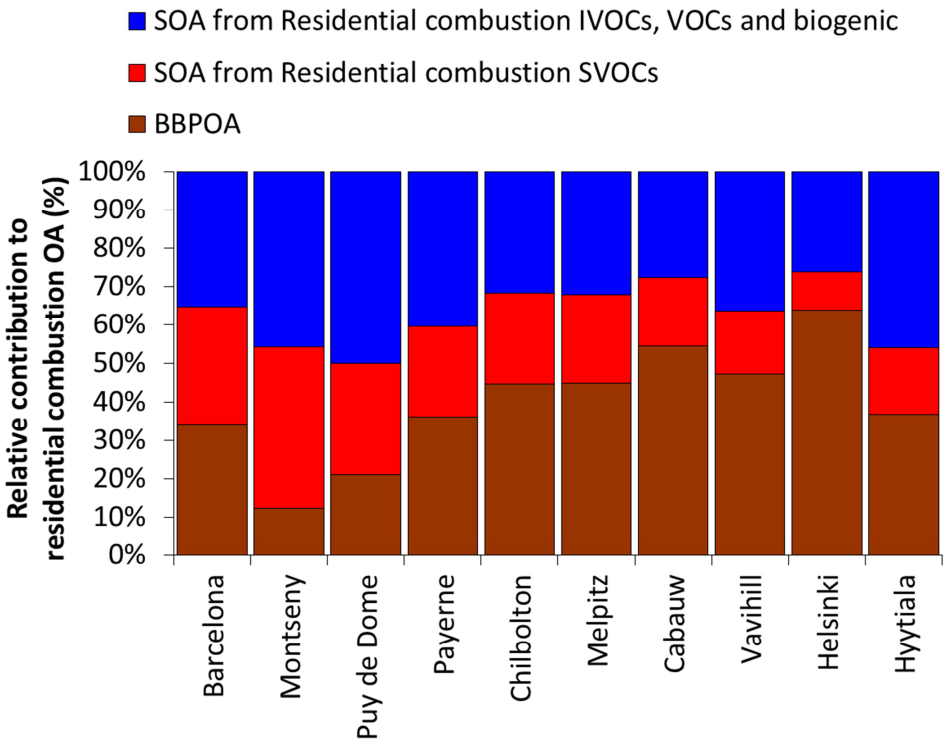

784

785 Figure 11. Contribution of residential and non-residential combustion precursors to SOA at
786 different sites (upper panel). Contribution of BBPOA, SVOCs and higher volatility organic
787 precursors to residential heating OA (lower panel). Stations are ordered from south to north.

788

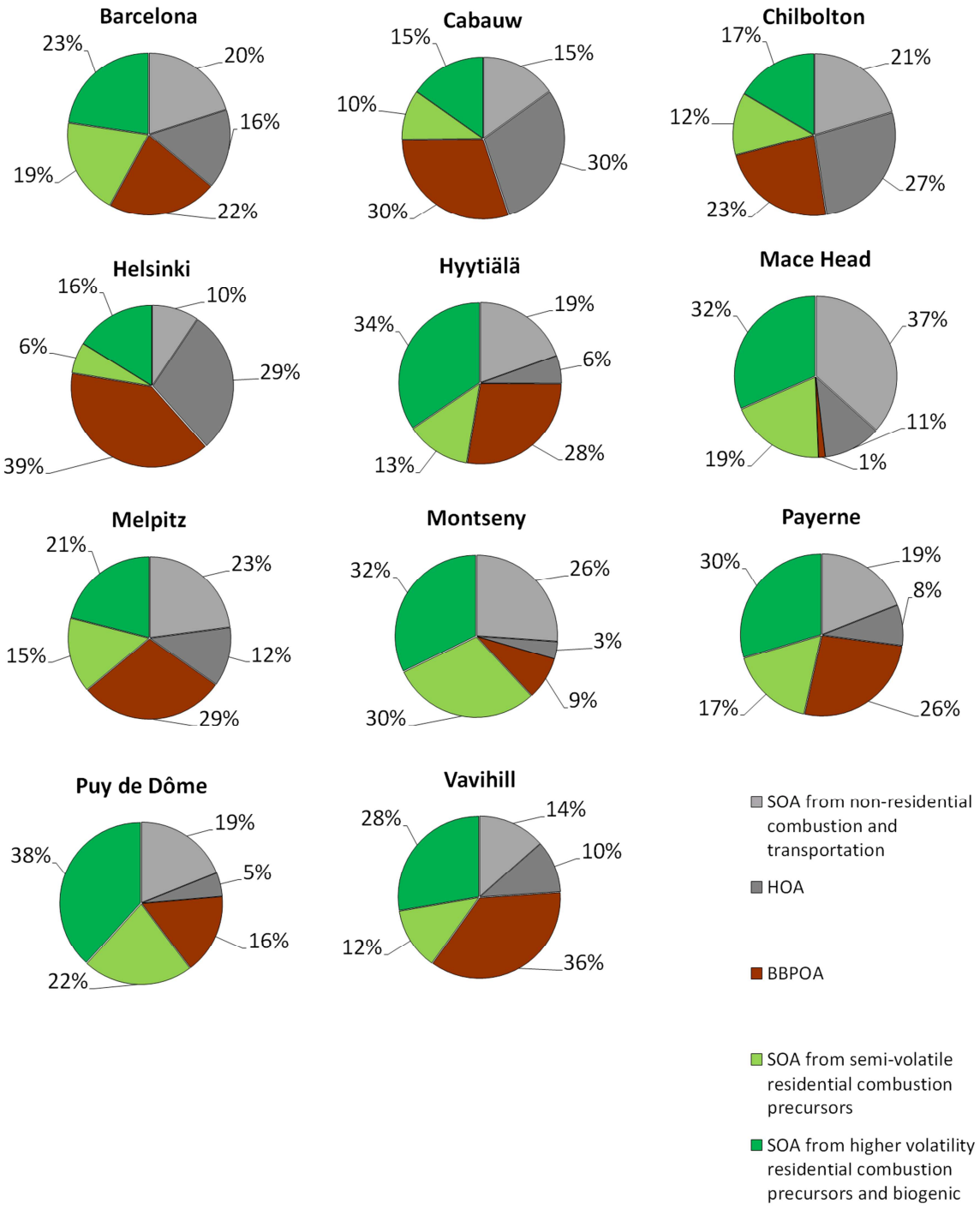

789

790 Figure 12. Average modelled composition of OA at the 11 AMS sites for the period between
791 25 February and 26 March 2009.

5 Supplement

Table S1. Statistics for model evaluation. M_i represents the modelled value, O_i the observations, $\overline{O}$ the mean of the observations and n the total number of data points.

Mean Bias (MB)	$MB = \frac{1}{n}\sum_{i=1}^{n}(M_i - O_i)$,
Mean Error (ME)	$ME = \frac{1}{n}\sum_{i=1}^{n}(\lvert M_i - O_i \rvert)$,
Mean Fractional Bias (ME)	$MFB = \frac{2}{n}\sum_{i=1}^{n}(\frac{M_i - O_i}{M_i + O_i})$,
Mean Fractional Bias (ME)	$MFE = \frac{2}{n}\sum_{i=1}^{n}(\frac{\lvert M_i - O_i \rvert}{M_i + O_i})$,
Coefficient of determination (R^2)	$R2 = 1 - \frac{\sum_{i}^{n}(O_i - M_i)^2}{\sum_{i}^{n}(O_i - \overline{O})^2}$.

Table S2. Statistical analysis for HOA during February-March 2009 periods at 11 AMS sites.

Site	Mean observed HOA ($\mu g\ m^{-3}$)	Mean modelled HOA ($\mu g\ m^{-3}$)	MB ($\mu g\ m^{-3}$)	ME ($\mu g\ m^{-3}$)	MFB [-]	MFE [-]	r	R^2
Barcelona	2.1	0.8	-1.3	1.5	-0.4	0.8	0.4	0.1
Cabauw	0.3	0.4	0.2	0.2	0.6	0.8	0.5	0.2
Chilbolton	0.5	0.3	-0.2	0.3	-0.5	0.7	0.8	0.6
Helsinki	0.4	1.0	0.6	0.7	0.8	0.9	0.2	0.1
Hyytiälä	0.0	0.1	0.1	0.1	0.7	0.8	0.6	0.3
Mace Head	0.1	0.1	-0.1	0.1	0.5	1.1	0.6	0.3
Melpitz	0.1	0.1	0.0	0.1	-0.1	0.6	0.6	0.3
Montseny	0.2	0.1	-0.1	0.2	-0.3	0.8	0.4	0.1
Payerne	0.3	0.3	-0.1	0.2	0.0	0.6	0.4	0.1
Puy de Dôme	0.0	0.1	0.0	0.0	0.3	0.8	0.1	0.0
Vavihill	0.4	0.2	-0.2	0.2	-0.4	0.7	0.5	0.2

Table S3 Statistical analysis for BBPOA during February-March 2009 periods at 11 AMS sites.

Site	Mean observed BBPOA ($\mu g\ m^{-3}$)	Mean modelled BBPOA ($\mu g\ m^{-3}$)	MB ($\mu g\ m^{-3}$)	ME ($\mu g\ m^{-3}$)	MFB [-]	MFE [-]	r	R^2
Barcelona	0.7	1.1	0.5	0.7	0.6	0.8	0.4	0.2
Cabauw	0.1	0.5	0.3	0.3	1.0	1.1	0.5	0.3
Chilbolton	0.5	0.2	-0.3	0.3	-0.6	0.8	0.6	0.4
Helsinki	0.4	1.4	1.0	1.1	1.1	1.1	0.1	0.0
Hyytiälä	0.1	0.5	0.4	0.4	1.5	1.5	0.7	0.5
Mace Head	0.3	0.0	-0.3	0.3	-0.9	1.4	-0.1	0.0
Melpitz	0.2	0.3	0.1	0.2	0.7	0.9	0.4	0.2
Montseny	0.2	0.3	0.1	0.2	0.5	0.8	0.2	0.1
Payerne	0.4	0.8	0.4	0.5	0.8	0.9	0.6	0.3
Puy de Dôme	0.1	0.2	0.1	0.2	0.5	1.0	0.3	0.1
Vavihill	0.7	0.7	0.1	0.5	-0.1	0.7	0.5	0.2

Table S4. Comparison of statistics for BBPOA in VBS_BC_NEW with VBS_BC (average of all sites in February-March 2009)

	Mean obs ($\mu g\ m^{-3}$)	Mean mod ($\mu g\ m^{-3}$)	MB ($\mu g\ m^{-3}$)	ME ($\mu g\ m^{-3}$)	MFB [-]	MFE [-]
VBS_BC	0.36	0.60	0.24	0.45	0.47	0.98
VBS_BC_NEW	0.36	0.59	0.23	0.43	0.50	0.97

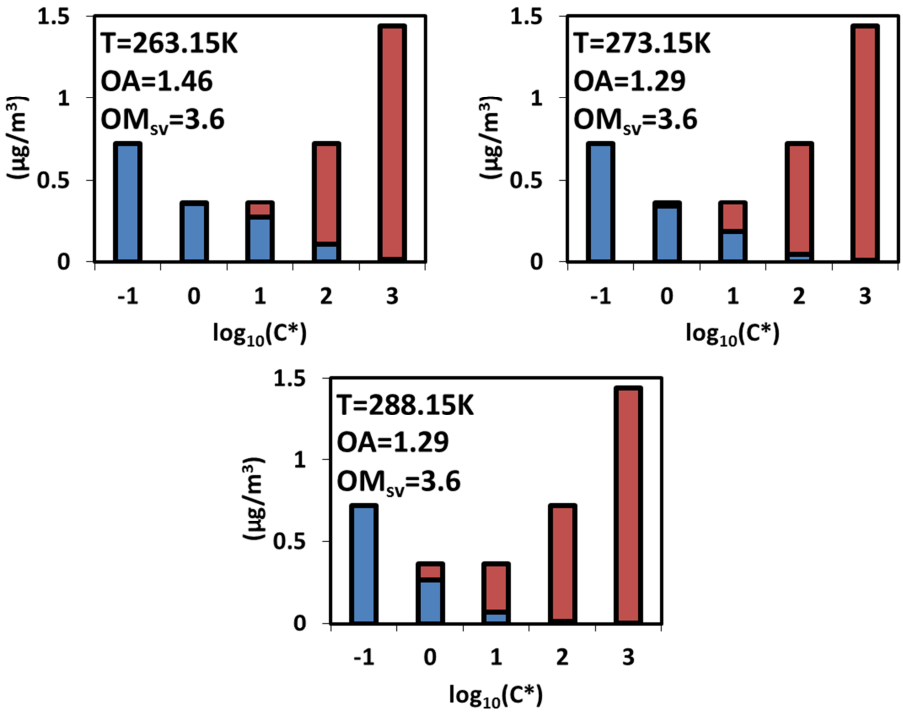

Figure S1. Box-model partitioning of biomass burning POA at about 1 µg m^{-3} OA at different temperatures (263.15, 273.15 and 288.15 K) using volatility distributions proposed by May et al. (2013). Particle phase is represented blue and gas phase in red. The lowest bin ($log_{10}C^{*}$=-1) is used as a proxy for all non-volatile species which will only reside in the particle phase.

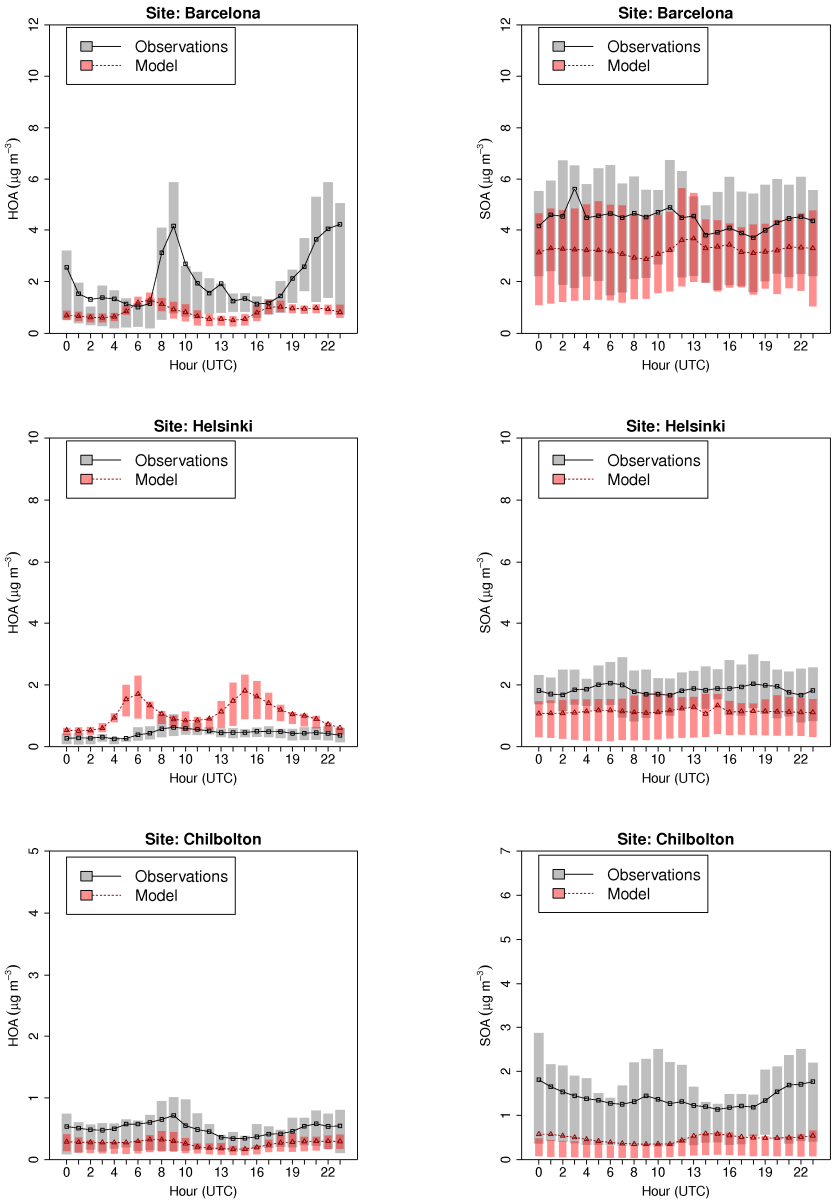

Figure S2. Comparison of modelled (red) and measured (grey) HOA and SOA diurnal profiles at the sites of Barcelona, Helsinki and Chilbolton. The extent of the bars indicates the 25th and 75th percentiles.

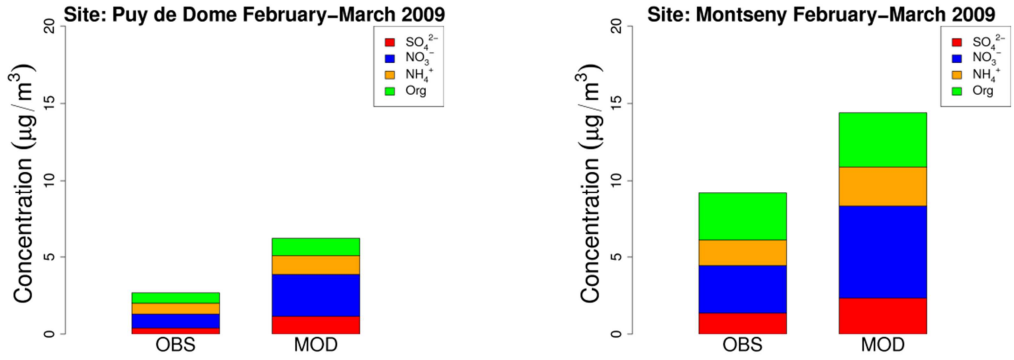

Figure S3. Comparison of modelled non-refractory PM25 components at Puy de Dome and Montseny with the AMS measurements in February-March 2009.

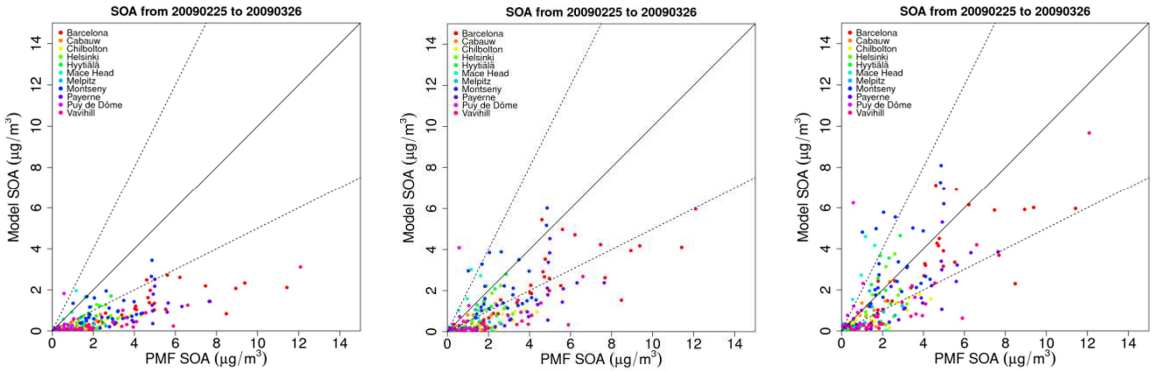

.

Figure S4. Modelled versus PMF SOA; with VBS _BC (Ciarelli et al., 2016a) (left panel), with VBS_BC where BBPOA vapours were allowed to be further oxidized (Koo et al. 2014) (middle panel), and with VBS_BC_NEW (right panel).

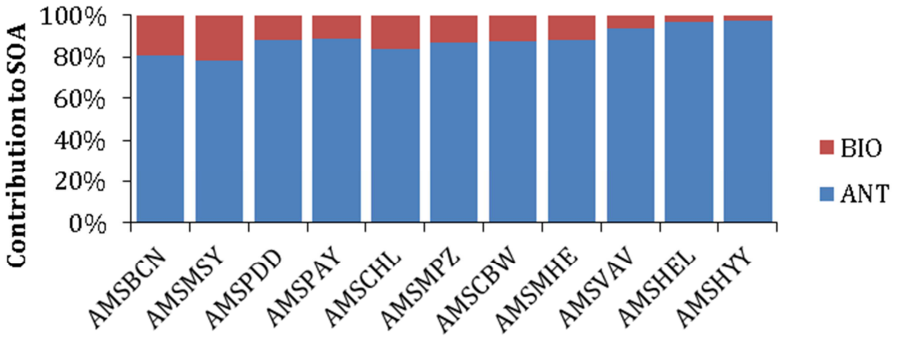

Figure S5. Biogenic and anthropogenic contribution to SOA at stations from south to north retrieved as a difference between the predicted SOA in the reference simulation (including biogenic) and a sensitivity test with no biogenic SOA formation.

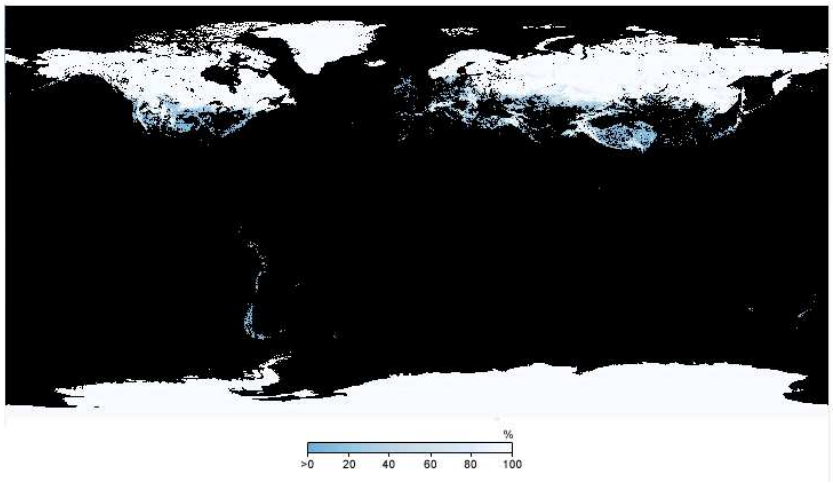

Figure S6. Snow cover for March 2009 as retrieved bythe TERRA/MODIS instrument.

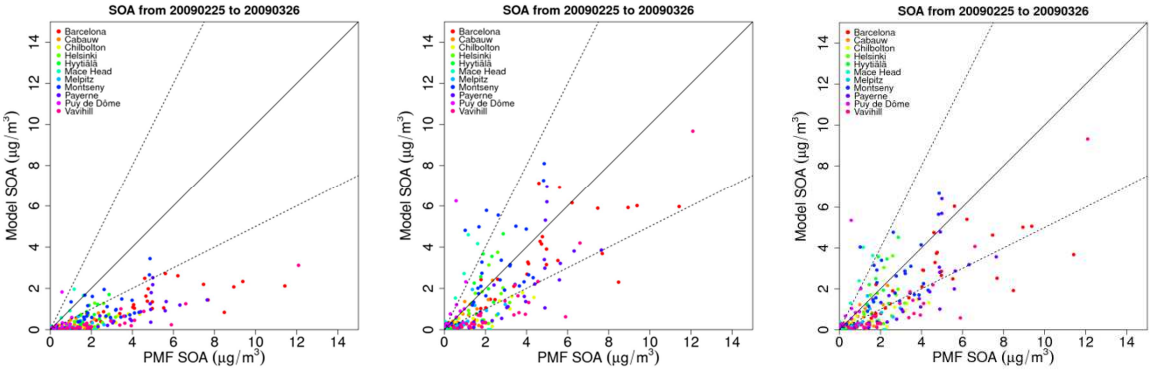

Figure S7. Modelled versus PMF SOA; with VBS _BC (Ciarelli et al., 2016a) (left panel), with VBS_BC_NEW (middle panel), and with VBS_BC_NEW but without biogenic SOA (right panel).